Renewable and Sustainable Energy Reviews 162 (2022) 112413

Contents lists available at ScienceDirect

Renewable and Sustainable Energy Reviews

journal homepage: www.elsevier.com/locate/rser

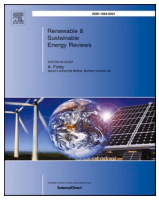

Recent advancements in sustainable upcycling of solid waste into porous carbons for carbon dioxide capture

Xiangzhou Yuan [a,b], Junyao Wang [c], Shuai Deng [d], Manu Suvarna [e], Xiaonan Wang [f], Wei Zhang [g], Sara Triana Hamilton [h], Ammar Alahmed [i], Aqil Jamal [i], Ah-Hyung Alissa Park [h], Xiaotao Bi [j,**], Yong Sik Ok [a,*]

[a] *Korea Biochar Research Center, APRU Sustainable Waste Management Program & Division of Environmental Science and Ecological Engineering, Korea University, Seoul, 02841, Republic of Korea*
[b] *R&D Centre, Sun Brand Industrial Inc, Jeollanam-do, 57248, Republic of Korea*
[c] *School of Materials and Energy, Guangdong University of Technology, Guangzhou, 510006, China*
[d] *Key Laboratory of Efficient Utilization of Low and Medium Grade Energy (Tianjin University), Ministry of Education of China, Tianjin, 300350, China*
[e] *Department of Chemical and Biomolecular Engineering, National University of Singapore, Singapore, 117585, Singapore*
[f] *Department of Chemical Engineering, Tsinghua University, Beijing, 100084, China*
[g] *Institute of Environmental Research at Greater Bay Area; Key Laboratory for Water Quality and Conservation of the Pearl River Delta, Ministry of Education, Guangzhou University, Guangzhou, 510006, China*
[h] *Department of Earth and Environmental Engineering and Department of Chemical Engineering, And the Lenfest Center for Sustainable Energy, The Earth Institute, Columbia University, New York, NY, 10027, USA*
[i] *Research and Development Center, Saudi Aramco, Dhahran, 31311, Saudi Arabia*
[j] *Department of Chemical and Biological Engineering and Clean Energy Research Centre, The University of British Columbia, 2360 East Mall, Vancouver, British Columbia, V6T 1Z3, Canada*

A R T I C L E I N F O

Keywords:
Life-cycle assessment
Machine learning
Sustainable development goal
Low carbon technology
Carbon neutral
Circular economy

A B S T R A C T

Carbon capture technologies have been extensively investigated as indispensable tools for reducing CO_2 emissions. In particular, CO_2 capture using solid waste-derived porous carbons (SWDPCs) has attracted significant research attention as one of the most promising and sustainable approaches to simultaneously mitigate climate change and address solid waste management challenges. Considerable research has recently been conducted on the thermal and chemical treatments of solid waste for upcycling into porous carbons (PCs) for effective and selective CO_2 capture. In this review, we discuss the synergistic benefits of employing SWDPCs for CO_2 capture and introduce innovative approaches for converting solid waste into PCs with the desired physical and chemical properties. The performance of SWDPCs for CO_2 capture is comprehensively discussed in terms of the synthesis route, CO_2 capture capacity, process cyclability, and sample optimization guided by machine learning. Furthermore, the mechanisms of CO_2 capture on PCs are discussed based on pore structures and incorporated surface functional groups. The life-cycle environmental impact of the PCs synthesized from solid waste and their practical applications for CO_2 capture are also evaluated. The overall environmental benefits of the proposed SWDPC-based CO_2 capture approach are analyzed in relation to the United Nations Sustainable Development

Abbreviations: BET, Brunauer–Emmett–Teller; CCUS, CO_2 capture, utilization, and sequestration; CED, cumulative energy demand; COF, covalent organic framework; COVID-19, coronavirus disease 2019; DL, deep learning; DNN, deep neural network; ESA, electricity swing adsorption; FU, functional unit; GBDT, gradient boosting decision trees; GCMC, grand canonical Monte Carlo; GWP, global warming potential; HTC, hydrothermal carbonization; IAST, ideal adsorbed solution theory; IL, ionic liquid; IPCC, Intergovernmental Panel on Climate Change; LCA, life-cycle assessment; LGB, light gradient boost; MDA, mean decrease in accuracy; ML, machine learning; MOF, metal–organic framework; MSW, municipal solid waste; NETL, National Energy Technology Laboratory; NOHM, nanoparticle organic hybrid material; PC, porous carbon; PET, polyethylene terephthalate; PSA, pressure swing adsorption; SEPAC, specific energy penalty of avoided CO_2; SWDPCs, solid waste-derived porous carbons; TGA, thermogravimetric analysis; TMP, thermodynamic molecular pump; TSA, temperature swing adsorption; UN SDG, United Nations Sustainable Development Goal; VSA, vacuum swing adsorption; VTCSA, vacuum/temperature/concentration swing adsorption; WMO, World Meteorological Organization; XGB, extreme gradient boost.

* Corresponding author.
** Co-corresponding authors.
E-mail addresses: tonybi@mail.ubc.ca (X. Bi), yongsikok@korea.ac.kr (Y.S. Ok).

https://doi.org/10.1016/j.rser.2022.112413
Received 28 September 2021; Received in revised form 8 March 2022; Accepted 28 March 2022
Available online 13 April 2022

Goals. Furthermore, the remaining challenges in upcycling solid waste into high-performance CO_2 adsorbents are discussed, and potential solutions are proposed.

1. Introduction

1.1. Climate change and carbon capture, utilization, and storage

Excessive greenhouse gas (such as CO_2) emissions, one of the most intractable environmental issues, have attracted the attention of both academia and industry. The ever-increasing atmospheric CO_2 concentration has exceeded 410 ppm [1], which is directly associated with fossil fuel combustion, and is considered to be the primary anthropogenic climate change driver [1–4]. With fossil fuels being the main energy source worldwide, atmospheric CO_2 concentration is predicted to continue increasing, potentially reaching a dangerous level of 550 ppm by 2050 [4,5]. In the absence of effective control, a typical 500 MW coal-fired power plant annually emits approximately 3 million tonnes of CO_2 into the atmosphere [5]. Moreover, the World Meteorological Organization (WMO) reported that the socioeconomic impacts of climate change are accelerating, and the physical manifestations of climate change are becoming more evident as unprecedented greenhouse gas concentrations drive global temperatures toward increasingly dangerous levels [6]. The Intergovernmental Panel on Climate Change (IPCC) has also reported the expected adverse impacts of a global temperature rise of 1.5 °C above pre-industrial levels [7], calling for more effective and efficient actions to prevent the threats arising from climate change due to anthropogenic activities. Moreover, in March 2021, the United Nations reported that human beings are running out of time to deliver the Paris Agreement and 2030 Agenda for Sustainable Development [8]. Therefore, CO_2 capture, utilization, and sequestration (CCUS) has been recognized as an indispensable approach in reducing CO_2 emissions from large point sources into the atmosphere. In addition to the paradigm shift to a renewable-energy-driven carbon-neutral society, the rapid deployment of CCUS is urgently needed to meet carbon neutrality targets. With the current coronavirus disease 2019 (COVID-19) pandemic, the world is experiencing unusual CO_2 emission trends [9], and post-pandemic industrial and economic recovery may significantly impact global greenhouse gas emissions. Considering that the quantity of CO_2 removed to carbon neutrality far exceeds that of current CCUS technologies, the large-scale implementation of CCUS technologies should be considered as an effective approach to avoid the unpredictable consequences of climate change.

Pre-combustion, post-combustion, and oxy-fuel combustion are the three main routes to capture CO_2 from large point emission sources, with post-combustion capture being the most promising and cost-effective route to date [10]. However, owing to the relatively low CO_2 concentration in post-combustion flue gases (e.g., 8–15%), the main challenge in this process is to develop a green and cost-effective CO_2 capture method. For post-combustion CO_2 capture, well-commercialized absorption processes (e.g., the regenerative amine process) are still considered expensive and pose issues, including solvent loss, critical corrosion, and environmental toxicity [11,12]. Although research is ongoing to address the challenges associated with amine-based solvents, attempts have also been made to develop novel solvents, including water-less and water-lean solvents, such as ionic liquids (ILs) and nanoparticle organic hybrid materials (NOHMs) [13–16]. In addition to solvent-based technologies, the development of low-cost membranes with high CO_2 permeability to capture CO_2 from flue gas is in progress. However, these technologies are unavailable for affordable commercial application.

CO_2 adsorption by solid adsorbents is also considered a promising carbon capture method because of its advantages of cost-effectiveness, well-developed pore structure, low energy requirement for regeneration (regeneration can be accomplished even by low-grade renewable solar thermal energy), and excellent cyclic stability [2,3,5,17–20]. In particular, solid waste-derived porous carbons (SWDPCs) are considered promising candidates for post-combustion CO_2 capture, and the upcycling of solid waste into value-added porous carbons (PCs) with high-performance CO_2 capture can significantly reduce the investment in carbon precursors for CO_2 adsorbents. Furthermore, such an approach could mitigate climate change caused by CO_2 emissions and environmental pollution resulting from inappropriate solid waste management.

1.2. Upcycling carbonaceous solid waste into CO_2-capture materials

An estimated 2.01 billion tonnes of solid waste is generated annually, which is expected to increase to 3.40 billion tonnes by 2050. Furthermore, the CO_2-equivalent greenhouse gas emissions generated by solid waste are expected to increase to 2.60 billion tonnes by 2050 [21]. The predominant sources of solid waste include construction and demolition, commercial and industrial waste, and municipal solid waste (MSW) [22]. An assessment of the global waste composition in 2018 revealed that the three largest waste categories were food and green waste (44%), paper and cardboard (17%), and plastic waste (12%) [21]. Such solid waste materials are carbon-rich resources and can be used as potential carbon precursors for carbon-based CO_2 adsorbents. Therefore, numerous researchers have valorized solid waste into PCs to mitigate CO_2 emissions, which is beneficial for achieving sustainable waste management guided by the concept of circular economy [23].

Herein, the application of major solid waste sources, such as food waste, plastic waste, MSW, forestry and agricultural waste, sewage sludge, animal waste, and industrial waste, in the development of CO_2 adsorbents is comprehensively discussed. Environmental pollution caused by plastic waste, such as micro- and nano-plastics, has recently attracted increasing attention [24–30], and all findings suggest that significant efforts should be dedicated to prevent this problem from escalating further [31]. This ubiquitous plastic pollution, particularly exacerbated by COVID-19 [32], has been labeled as an important driver of global environmental change owing to the very high levels of energy and resources utilized to synthesize plastic polymers, inevitable biogeochemical cycling of used plastic products, and subsequent direct and indirect impacts of micro- and nano-plastics on ecosystems [25]. Considering the plastic cycle proposed by Bank et al. [25] and the major types of particulate plastics (cosmetic microbeads and fragments derived from the breakdown of large plastic debris) in most ecosystems [33], upcycling plastic waste into PCs could be an effective and sustainable method for preventing the generation of microplastics from plastic debris. Therefore, the upcycling of solid plastic waste into CO_2 adsorbents is highlighted in this review with the aim of understanding and designing solid waste-derived CO_2 adsorbents and sustainable waste management by researchers in relevant fields, thereby promoting the development of solid waste-based technologies for practical applications.

1.3. Challenges and opportunities

As presented in Table 1, in 2012, Olivares–Marin and Maroto–Valer [2] published the first review on the synthesis and use of CO_2 adsorbents derived from waste precursors, such as coal byproducts (fly ash, bottom ash, and unburned carbon in fly ash), biomass products (agricultural residues), water treatment byproducts (sludge cake), and household residues (packaging waste). Since then, this topic has attracted increasing attention. Wang et al. reviewed solid CO_2 adsorbents based on their working temperatures (i.e., low temperature [< 200 °C], intermediate temperature [200–400 °C], and high temperature [>

400 °C]) in 2014 [3]; in 2019, they reviewed solid waste-derived CO_2 adsorbents (i.e., carbon-based, silica-based, silicate-based, calcium--based) [18]. In 2020, Dissanayake et al. [34] summarized and evaluated the potential of using pristine and engineered biochar as CO_2 capture media, factors influencing the CO_2 adsorption capacity of biochar, and issues related to the synthesis of biochar-based CO_2 adsorbents. Further studies are recommended to develop cost-effective and sustainable biochar-based composites for large-scale CO_2 capture. As summarized in Table 1, previous reviews have primarily focused on biomass and industrial waste-derived CO_2 adsorbents prepared by carbonization/activation and related surface modifications, which were only evaluated from the perspective of CO_2 adsorption performance (i.e., CO_2 uptake, cyclic stability, selectivity, and adsorbent regeneration).

Solid waste is considered to provide a versatile and efficient platform for the synthesis of PCs. This has led to a considerable shift in research interest toward different potential applications of solid waste, including CO_2 capture. Fig. 1 shows a scientometric visualization of the top 300 keywords of 2187 peer-reviewed publications within the database of "Web of Science Core Collection," using "CO_2 capture" and "waste" as the search keywords (topic). The results from such studies imply that a) adsorption has been widely considered a promising route for CO_2 capture, and b) compared to zeolite-, cellulose-, and CaO-based sorbents, solid waste-derived activated carbons/PCs have been extensively applied for synthesizing CO_2 adsorbents in the last few years. As shown in Fig. 2a, a solid waste-based CO_2 capture route has been commonly developed, including the synthesis of PC and CO_2 adsorption from the perspectives of both isotherms and kinetics, suggesting that it is time-consuming without considering the sustainability of the entire process. Moreover, current data-driven approaches such as machine learning (ML) have been applied to guide and optimize the synthesis of high-performance SWDPCs for CO_2 capture [42]. The environmental impact and feasibility of SWDPC-based CO_2 capture processes are still unclear with regard to industrial applications and should be comprehensively evaluated to clarify whether these processes are closed carbon loops and beneficial for achieving carbon neutrality. Therefore, it is necessary to provide a timely and comprehensive review of SWDPCs for CO_2 capture, including the advanced synthesis of high-quality PCs from solid waste, detailed SWDPC-based CO_2 capture performance evaluations and potential adsorption mechanisms, ML-guided optimization of SWDPCs for CO_2 capture, systematic environmental impact assessment from a life-cycle perspective, and concluding remarks and future perspectives (Fig. 2b). This review sheds light on the design and optimization of solid waste-based adsorbents and ultimately promotes their large-scale deployment for CO_2 capture, which may be beneficial to researchers and policymakers working in the areas of sustainable waste management, climate change mitigation, and carbon circular economy. To achieve the United Nations Sustainable Development Goals (UN SDGs) by 2030, solid waste management and climate change mitigation should be performed in a sustainable manner based on the takeaways from this comprehensive review.

2. Technological advancements in upcycling solid waste into porous carbons

The conversion of solid waste to PCs with excellent CO_2 adsorption performance has recently been investigated, with a focus on optimizing the textural properties and increasing the CO_2 selectivity via activation and surface modification, respectively (Fig. 2b).

2.1. Production of biochars and hydrochars from carbonaceous solid waste

Thermochemical conversion methods, including pyrolysis, hydrothermal carbonization (HTC), gasification, and ionothermal

Table 1
Overview of solid waste-derived CO_2 adsorbents in previous reviews.

	Major solid carbon waste			Porous carbon synthesis		Performance evaluation		System optimization	Environmental impact
	Biomass waste	Plastic waste	Industrial waste	Carbonization and activation	Surface modifications	CO_2 adsorption performance[a]	Cyclic performance[b]	AI (i.e., ML, DL)[c]	Life-cycle assessment
Olivares–Marin and Maroto–Valer (2012) [2]	✓		✓	✓	✓	✓			
Kaithwas et al. (2012) [35]			✓	✓	✓	✓			
Wang et al. (2014) [3]	✓		✓	✓		✓			
Lee et al. (2015) [36]	✓		✓	✓		✓			
Rashidi et al. (2016) [37]	✓			✓	✓	✓			
Creamer et al. (2016) [19]	✓			✓		✓			
Zhao et al. (2018) [38]	✓		✓	✓	✓	✓			
Singh et al. (2019) [39]	✓			✓	✓	✓			
Wang et al. (2019) [18]	✓		✓	✓	✓	✓			
Dissanayake et al. (2020) [34]	✓			✓		✓			
Ochedi et al. (2020) [17]	✓			✓	✓	✓			
Zhou et al. (2020) [40]	✓			✓		✓			
Li et al. (2021) [41]	✓			✓	✓	✓	✓		
This review	✓	✓	✓	✓	✓	✓	✓	✓	✓

[a] CO_2 adsorption performance was evaluated with respect to CO_2 uptake, cyclic stability, selectivity, and adsorbent regeneration.
[b] Cyclic performance was evaluated via temperature swing adsorption (TSA), pressure swing adsorption (PSA), electricity swing adsorption (ESA), and temperature/vacuum swing adsorption (TVSA) using key indicators (purity, recovery, productivity, and working capacity).
[c] AI, ML, and DL represent artificial intelligence, machine learning, and deep learning, respectively.

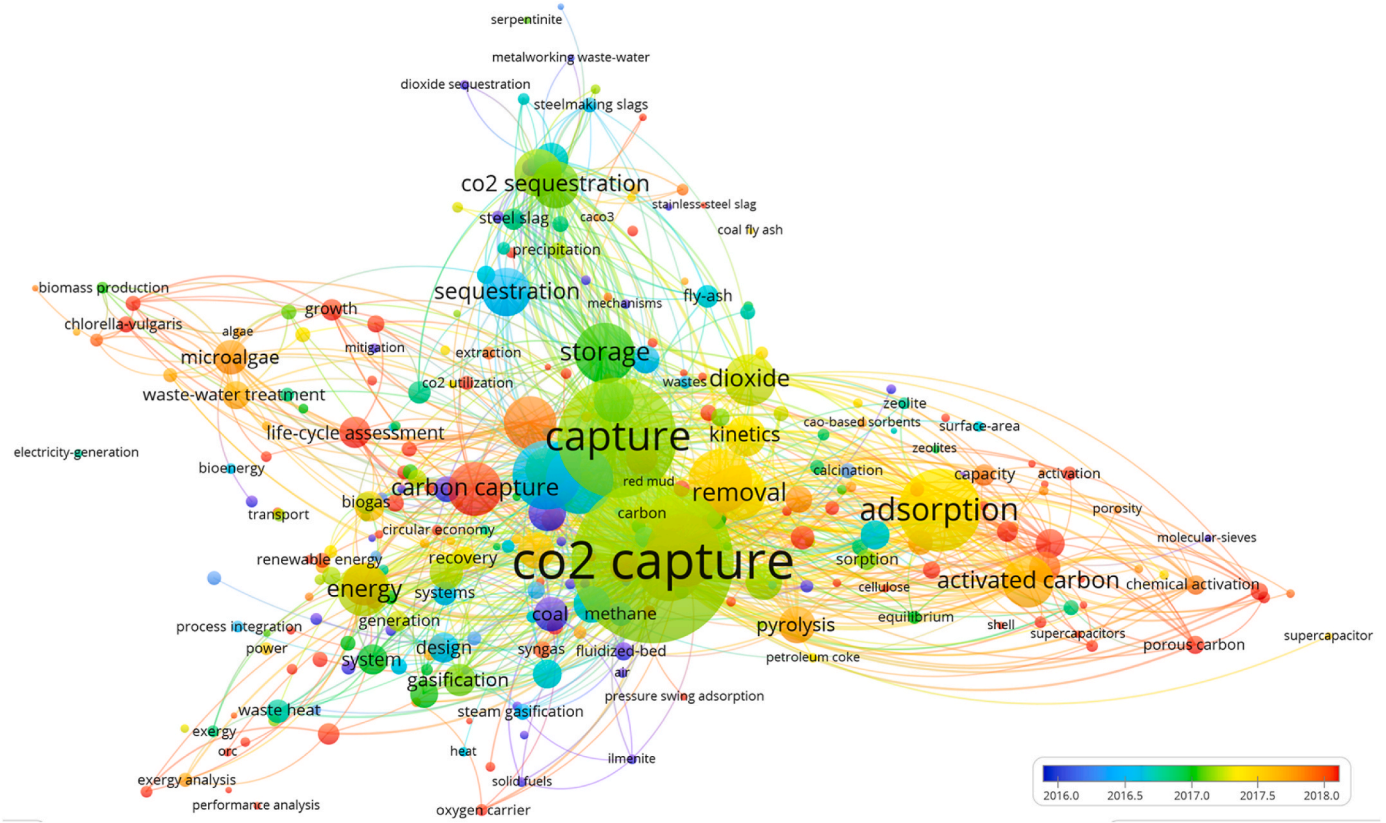

Fig. 1. Scientometric visualization of the top 300 keywords of all peer-reviewed publications released from 1995. A total of 2187 publications were retrieved from the Web of Science with "CO_2 capture" and "waste" as the search keywords (topic). The "Web of Science Core Collection" was the selected database. Collected data were analyzed using the built-in function of co-occurrence of all keywords and plotted in "overlay visualization" using VOSviewer. Each circle stands for a keyword, while its size represents the number of times a pair of keywords co-occurred in the publications. The legend with different colors represents the average year of occurrence of each keyword.

carbonization, can be used to convert solid waste into PCs, followed by physical or chemical activation [43–45]. Pyrolysis and HTC are considered the most promising methods for solid waste valorization [46,47]; they are environment-friendly and cost-effective [19,43,44], and hence, they have attracted the interest of many researchers. Biochar and hydrochar are typically generated via pyrolysis and HTC, respectively, and PC is upgraded from biochar/hydrochar via physical and/or chemical activation. Additional details are presented in Table 2. Pyrolysis is an important method for the reduction and valorization of solid waste into value-added products, such as biochar, bio-oil, and bio-syngas, over a wide temperature range (e.g., 300–900 °C).

Depending on the heating rate, residence time, and heating type, pyrolysis can be classified into slow, fast, flash, and microwave-assisted processes [48–52]. Pyrolysis presents two major advantages: a) it can be optimized for the desired products; specifically, slow pyrolysis (heating rate $< 50\ ^{\circ}C\ min^{-1}$) increases the biochar yield, whereas fast pyrolysis is more suitable for producing bio-oils; and b) it is flexible as it can be used for different feedstock types and is operational under a wide range of conditions [48]. HTC is considered a promising alternative route to dry thermochemical processes (e.g., pyrolysis and gasification) because it does not require drying pretreatment, is cost-effective, and requires mild operating conditions (180–265 °C) [53]. Owing to the different reaction media used in pyrolysis and HTC, the physical and chemical properties of biochar and hydrochar are significantly different [54,55].

2.2. Surface activation of chars to prepare porous carbon with optimal porosity

Because biochar and hydrochar are associated with poor textural properties (low surface area, undeveloped pore structure, and unspecified functional groups; see Table 2), their performance in specific applications is limited. Therefore, both physical and chemical activations, as well as surface modification of biochar and hydrochar to further improve their physical and chemical properties and expand their application areas, have attracted increasing attention [56–59]. SWDPCs obtained after activation and/or surface modification are considered cost-effective and environment-friendly carbon materials with high porosity and effective functional groups, which are beneficial to CO_2 adsorption [39,57,60,61].

Physical and chemical activations at high temperatures are considered as effective and efficient approaches for producing PCs with high porosity. Steam, CO_2, air, or mixtures of these are widely used as physical activation agents [57,62]. CO_2 is the most commonly used activation agent and is based on theoretical thermodynamic calculations of the Boudouard reaction (Eq. (1)); the operating temperature exceeds 700 °C. Fang et al. [63] reported that the surface area and pore volume of biochar increase with increasing operating temperature and activation time. Physical activation is relatively green but commonly operates in the high-temperature range of 500–900 °C, particularly when steam is combined with a purging gas, and the corresponding PC yield is low, which causes the number of O-containing functional groups on the surface of PCs to decrease [64]. The chemical reactions that occur during CO_2 or steam activation can be described by Eqs. (1)–(3) [43], indicating that physical activation occurs at high temperatures. In addition, the surface area of some PCs can be smaller than 1000 $m^2\ g^{-1}$, and the PC material yield can be lower than 30% after physical activation.

$$C + CO_2 \rightarrow 2CO,\ \Delta H = 159\ kJ\ mol^{-1} \quad (1)$$

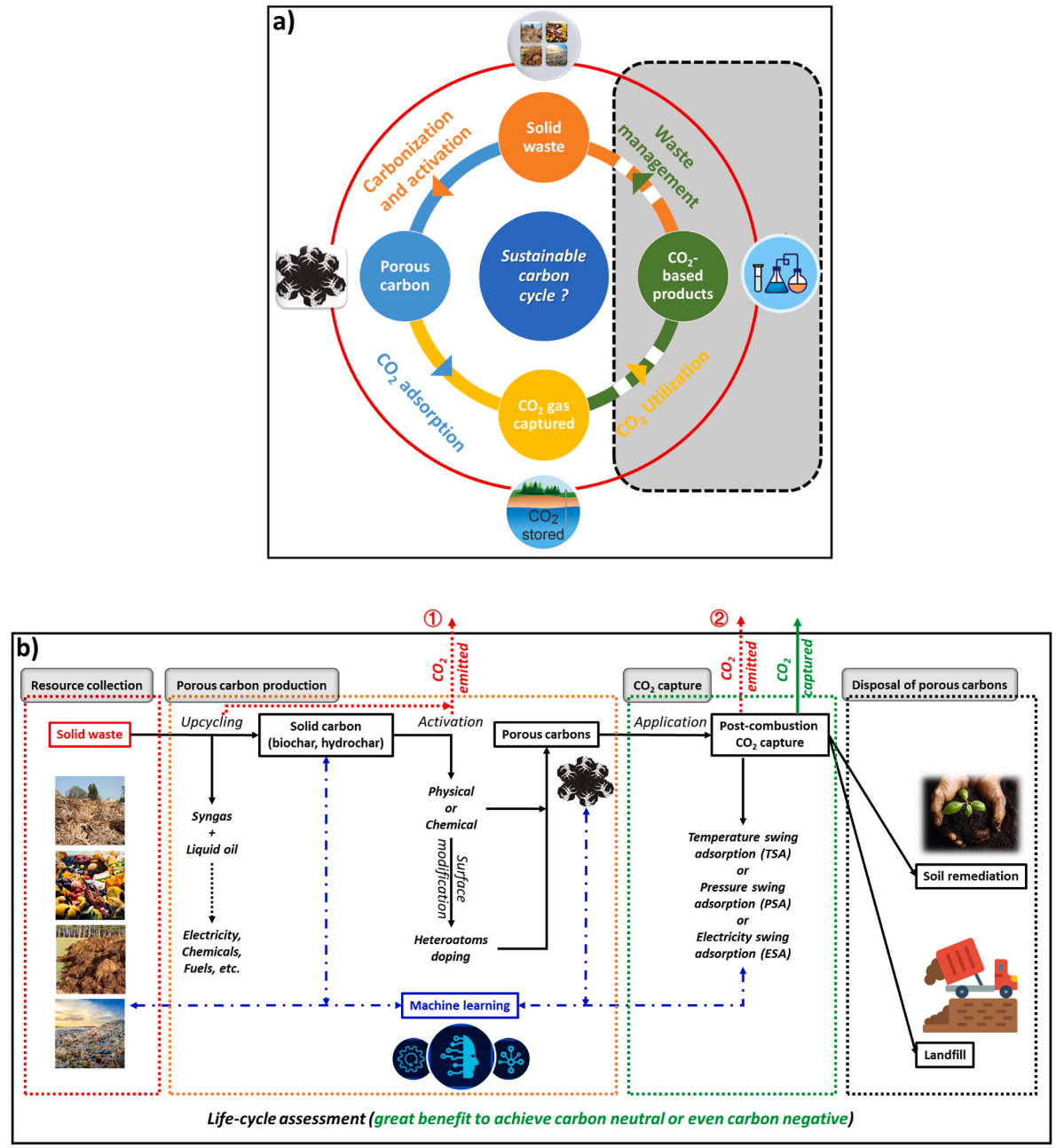

Fig. 2. a) General solid waste-based CO_2 capture route (the CO_2 utilization in gray dashed section is not discussed here), and b) circular economy-inspired sustainable upcycling of solid waste into desired porous carbons for post-combustion carbon dioxide (CO_2) capture.

$$C + H_2O \rightarrow CO + H_2,\ \Delta H = 117\ kJ\ mol^{-1} \quad (2)$$

$$CO + H_2O \rightarrow CO_2 + H_2,\ \Delta H = 41\ kJ\ mol^{-1} \quad (3)$$

where ΔH is the enthalpy of reaction.

H_3PO_4, KOH, NaOH, K_2CO_3, and $ZnCl_2$ are the typical chemical activation agents. Owing to its low operating temperature and short duration, chemical activation involves lower energy consumption and produces a higher yield of PCs with well-developed pore structures than physical activation [65–67]. KOH is considered the most promising and effective chemical activation agent for developing ultra- and micro-pore structures. The detailed mechanism for increasing the porosity via KOH activation is as follows [43,66].

$$2KOH + CO_2 \rightarrow K_2CO_3 + H_2O \quad (4)$$

$$2C + 2KOH \rightarrow 2CO + 2K + H_2 \quad (5)$$

$$K_2CO_3 + C \rightarrow K_2O + 2CO \quad (6)$$

$$K_2O + C \rightarrow 2K + CO \quad (7)$$

Sun et al. [68] reported that the specific surface area and total pore volume of sunflower-derived PC activated by KOH are 3072 $m^2\ g^{-1}$ and 1.77 $cm^3\ g^{-1}$, respectively. Wei et al. [69] reported that the specific surface area and total pore volume of a water chestnut-based PC activated by KOH were 3401 $m^2\ g^{-1}$ and 2.50 $cm^3\ g^{-1}$, respectively. These results suggest that chemical activation plays a significant role in the synthesis of high-quality PCs. The porosity of the synthesized PCs depends not only on the activation routes and operating conditions but also on the properties of solid waste used. Chemical activation has been widely recommended for preparing high-quality PCs owing to its short

Table 2
Solid waste-derived products from various preparation methods.

	Solid waste	Biochar/ hydrochar	Porous carbon
Carbon content (%)	15–80	40–90	80–95
Preparation method	Drying pretreatment	Pyrolysis or hydrothermal process	Pyrolysis or hydrothermal process followed by physical or chemical activation
Effective functional groups	few	few	numerous
Surface area ($m^2\ g^{-1}$)	n.a.	$\leq$ 800	$\geq$ 1000
Total pore volume ($cm^3\ g^{-1}$)	n.a.	$\leq$ 0.3	$\geq$ 0.5

reaction time and low operating temperature. However, equipment corrosion and wastewater treatment should be carefully considered because of the use of chemical agents.

2.3. Functionalization of porous carbon for CO_2 capture

Surface modification has been widely considered as one of the most effective and promising routes to enhance the CO_2 capture capacity and selectivity over other gases (i.e., N_2 co-existing in flue gas) because effective surface functional groups can provide more active sites for the adsorption of CO_2 molecules [42,39,45]. Heteroatom doping (e.g., with nitrogen, oxygen, and sulfur) and metal doping (e.g., with metal oxides, metal hydroxides, and metal oxyhydroxides) are widely used for surface modification to create more basic and/or active sites on the surfaces of the synthesized PCs.

2.3.1. N-doping treatment

Among the functional groups mentioned, nitrogen (N) is the most promising and widely used for synthesizing CO_2 adsorbents. Ammonia, zinc nitrate, sodium amide, urea, and melamine are commonly used to increase the N content of PCs. Ammonia, a common nitrogen source, has been extensively explored in recent decades for preparing nitrogen-containing PCs via thermal treatment (commonly called amination) to improve the adsorption performances [70–72]. During amination, NH_3 serves as both the activating agent and N source [71,72]. Specifically, ammonia decomposes at high temperatures to form radicals such as NH_2, NH, and H, which may react with the surface carbon to form functional groups such as –NH_2-, –CN, pyridinic, pyrrolic, and quaternary nitrogen [73,74]. Liu et al. [60] performed a single-step sodium amide ($NaNH_2$) activation process to improve the N functional groups in hazelnut shell-derived CO_2 adsorbents. In this single-step process, $NaNH_2$ acted as both an activator and nitridation, circumventing tedious and time-consuming processes for preparing *N*-doped PCs, making this kind of CO_2 adsorbent more cost-effective. Pyrrolic N, which has been verified as the most favorable N species for CO_2 adsorption, is the most functional N group compared to pyridinic N and quaternary nitrogen. Yuan et al. [66] investigated *N*-doping treatment using urea as the N source through one-pot synthesis; KOH and urea were used as the activator and nitridation source, respectively, to prepare high-quality CO_2 adsorbents at an activation temperature of 700 °C. The oxygen (O) content was increased during this one-pot synthesis, such as carbonyl oxygen atoms in esters and oxygen atoms in hydroxyls or ethers, which offer Lewis basic sites that are beneficial for CO_2 binding. Moreover, O atoms typically combine with C atoms to form acidic or basic functional groups on the surface. Notably, the decomposition of O-containing acidic functional groups can occur at a temperature of 800 °C [75]. Nitric acid (HNO_3), sulfuric acid (H_2SO_4), and hydrogen peroxide (H_2O_2) are widely used to generate O-rich functional groups on the surface of PCs [39].

2.3.2. Dual-doping treatment

In addition to single-doping treatment, dual-doping treatment has also been investigated to enrich surface functional groups. Nazir et al. [76] used thiourea as the N and S co-provider to prepare N and S co-doped PC from corn starch waste (Fig. 3a), reaching 4.6 at% of N and 2.3 at% S in the produced PC. Rehman et al. [77] used urea and thiourea to synthesize cellulose-based PCs (Fig. 3b) with varying contents of O (4.8–17.1 at%), N (3.2–10.1 at%), and S (1.9–3.6 at%) under different operating conditions. Moreover, several typical SWDPCs demonstrate

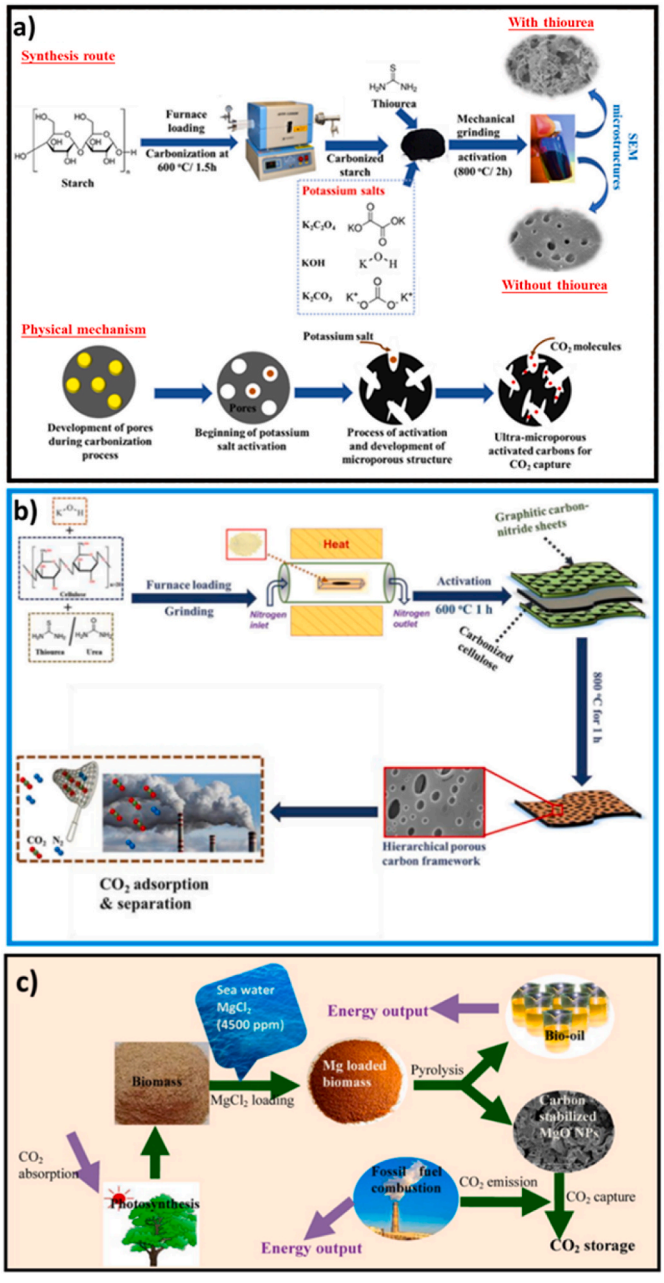

Fig. 3. a) Schematic of the step-by-step synthesis of undoped/N, S co-doped potassium salt-activated starch-derived microporous carbons (Reproduced with permission from Ref. [76]), b) synthetic protocol for N, S-doped microporous carbons for efficient CO_2 capture (Reproduced with permission from Ref. [77]), and c) schematic of the synthesis of mesoporous carbon stabilized magnesium oxide (MgO) nanoparticles (NPs) for CO_2 capture (Reproduced with permission from Ref. [84]).

high functional groups owing to their natural element availability; for example: 2.86 wt% N in shrimp shell-derived PC [78], 4.16 wt% N in pueraria-derived PC [79], 7.90 wt% N in celery-derived PC [80], 4.62 wt % N and 2.56 wt% S in willow catkin-derived PC [81], 4.94 wt% N and 1.12 wt% S in human hair-derived PC [82], and 1.5 wt% N, 0.5 wt% S, and 5.0 wt% O in ant powder-derived PC [83].

2.3.3. Metal-doping treatment

In continuing efforts to improve the CO_2 adsorption performance, metal-doping treatment has been considered because metal oxides, hydroxides, and oxyhydroxides are generally basic and tend to bond with acidic CO_2 molecules [85]. Lahijani et al. [85] reported that the incorporation of basic metal sites into walnut shell-based PCs effectively enhances CO_2 capture in the following order: Mg > Al > Fe > Ni > Ca > raw biochar > Na. The Mg-loaded sorbent was prepared using magnesium nitrate hexahydrate ($Mg(NO_3)_2{\cdot}6H_2O$), which underwent endothermic dehydration to anhydrous $Mg(NO_3)_2$ at approximately 110–190 °C. Anhydrous $Mg(NO_3)_2$ decomposes to magnesium oxide (MgO) at temperatures above 400 °C. The formation of basic MgO sites favors the adsorption of CO_2 via interactions with the basic O^{2-} ions of the $O^{2-}Mg^{2+}$ bonds, which facilitates the formation of carbonates [86,84]. Liu et al. [84] applied seawater, which is naturally abundant, in $MgCl_2$ (~0.45%) to synthesize the Mg-doped PCs (Fig. 3c) from sawdust with Mg loading contents of 19.4–21.1 wt%.

Thermochemical treatments, described in **Sections** 2.1, 2.2, and 2.3, can lead to secondary pollution; for example, heavy metal pollution occurs when $ZnCl_2$ and $Zn(NO_3)_2$ are used as chemical activation and surface modification agents, respectively, because washing with 10% HCl and/or distilled water is unavoidable after treatment with these compounds. Moreover, CO_2 emissions are inevitable from these thermochemical processes, implying that increasing attention should be paid to fully assess the life-cycle environmental impact of PC synthesis from solid waste.

2.4. CO_2 capture mechanisms of porous carbons

CO_2 adsorption on SWDPCs can occur via physical or chemical routes; however, the mechanism of CO_2 capture is largely dependent on the textural properties and surface chemistry [42,87]. The heat of adsorption (Q_{st}) has been widely considered as a key indicator for distinguishing physisorption- or chemisorption-dominated CO_2 adsorption; the Q_{st} is lower than 40 kJ mol^{-1} for physisorption, whereas it is higher than 40 kJ mol^{-1} (up to 800 kJ mol^{-1}) for chemisorption [88]. For regular PC (without surface modification), the results from existing studies indicate that the main mechanism for CO_2 adsorption is physisorption, primarily driven by van der Waals forces, implying the critical role of textural properties in the CO_2 capture process [19]. For example, Yuan et al. [67] and Choi et al. [89] reported that CO_2 adsorption on SWDPCs at 0.15 bar and 1 bar was primarily related to the pore volumes of narrow pores less than 0.6 nm and 0.8 nm in diameter, respectively. This suggests that there is no linear relationship between CO_2 uptake and total pore volume or between CO_2 uptake and specific surface area. Moreover, CO_2 molecules can be adsorbed on SWDPCs at low temperatures (lower than 75 °C) and high pressures and are desorbed at high temperatures (up to 150 °C) and low pressures, suggesting a low energy consumption for adsorbent regeneration.

In PCs modified with doping treatment (i.e., with surface activation), CO_2 adsorption could be governed by both chemisorption and physisorption, owing to the existence of effective functional groups. Surface chemistry is a critical factor in providing more active sites for CO_2 capture via chemisorption through effective bonding between CO_2 and the adsorbent surface (i.e., Lewis acid–base interactions). In the heteroatom (N, O, and S) doping treatment, the basic O functional groups of –OH and –COOH [67,90], N functional group of pyrrolic N [66], and S functional groups of oxidized S [91] are considered the most effective functional groups for improving the CO_2 adsorption performance. Metal (i.e., Mg, Fe, and Al) doping treatment could lead to the formation of chemical carbonates, causing an increase in CO_2 capture; here, physisorption and acid–base banding interactions play relatively minor roles in CO_2 capture. For example, as presented in Fig. 3c, Liu et al. [84] synthesized sawdust-derived PC-stabilized MgO nanoparticles (mPC–MgO) for CO_2 capture using $MgCl_2$ in low concentrations from seawater as the Mg metal source. In addition to the well-developed porous structure and basic –OH functional groups, the formation of $MgCO_3$ enhanced by the MgO crystal structure in a chemisorption-dominated manner primarily contributes to the excellent CO_2 adsorption performance. Moreover, the adsorption–desorption cycle was conducted at 80 °C to adsorb CO_2 molecules and at 500 °C to desorb CO_2 molecules.

3. CO_2 capture performance of solid waste-derived porous carbons

An ideal PC for CO_2 adsorption should exhibit excellent CO_2 adsorption capacity, high selectivity, stable recyclability, fast adsorption/desorption kinetics, and facile regeneration [87] (Fig. 4). These criteria are widely used to evaluate the CO_2 adsorption performance of PCs derived from solid waste. We summarized the suitable PCs for CO_2 adsorption and their performance retrieved from our literature survey in Table 3.

3.1. CO_2 capture working capacity

CO_2 adsorption capacity can be classified into dynamic and isothermal adsorption capacities. For SWDPCs, both CO_2 isothermal and dynamic adsorption capacities have been investigated in most existing studies. ASAP 2020, 2420, and 2460 (Micromeritics), Autosorb-iQ (Quantachrome), and 3H–2000PS2 (Beshide) sorption analyzers have been widely used to obtain isothermal CO_2 adsorption data. Thermogravimetric analysis (TGA) and vertical or horizontal fixed-bed reactors have been used to obtain dynamic CO_2 adsorption data. According to the National Energy Technology Laboratory (NETL) Technical Report, an adsorbent is applicable and practical for CO_2 capture when its isothermal CO_2 adsorption capacity exceeds 3 mmol g^{-1} at 25 °C and 1 bar [131]. As presented in Table 3, the CO_2 adsorption capacities of most PCs exceeded 3 mmol g^{-1} at 25 °C and 1 bar after effective carbonization, activation, and/or surface modification. This suggests that the valorization of solid waste into PCs for CO_2 capture could be a promising approach to simultaneously solve two environmental issues: (i) global warming caused by CO_2 emissions [28,29] and (ii) environmental pollution caused by the mismanagement of solid waste [66,67,92]. Yuan et al. [66,67,93] successfully upcycled waste polyethylene terephthalate (PET) plastic bottles into CO_2 adsorbents. The CO_2 adsorption capacities of the CO_2-activated (*PET6-CO_2-9*), KOH-activated (*PET–KOH–973*), and both KOH and Urea-modified (*PET6KN$_{one-pot}$*) adsorbents reached 3.63 mmol g^{-1} [93], 4.42 mmol g^{-1} [67], and 4.58 mmol g^{-1} [66], respectively, at 25 °C and 1 bar. The well-developed microporous structure of *PET–KOH–973* is illustrated in Fig. 5a and Fig. 5b, which shows that KOH activation was effective for micropore development. The CO_2 adsorption isotherms of *PET–KOH–973* revealed that *PET–KOH–973* is a promising candidate for CO_2 capture owing to its excellent CO_2 capture capacity (Fig. 5c). The CO_2 uptake of all the prepared samples exhibited good linear relationships with the cumulative pore volumes limited by narrow micropores smaller than 0.8 nm ($V_{0.8}$; $R^2 = 0.975$) (Fig. 5d). The experimental data further indicated that $V_{0.8}$ played a predominant role in CO_2 uptake by waste PET-derived PCs at 25 °C and 1 bar. In addition, the effect of pore size on CO_2 uptake was analyzed using the grand canonical Monte Carlo (GCMC) simulation (Fig. 5e), and the results were consistent with the experimental findings that a pore size of less than 0.8 nm is dominant in the CO_2 adsorption process, and the adsorption of CO_2 molecules increased when the pore size was approximately twice the kinetic diameter of CO_2 (i.e., 3.3 Å) [67].

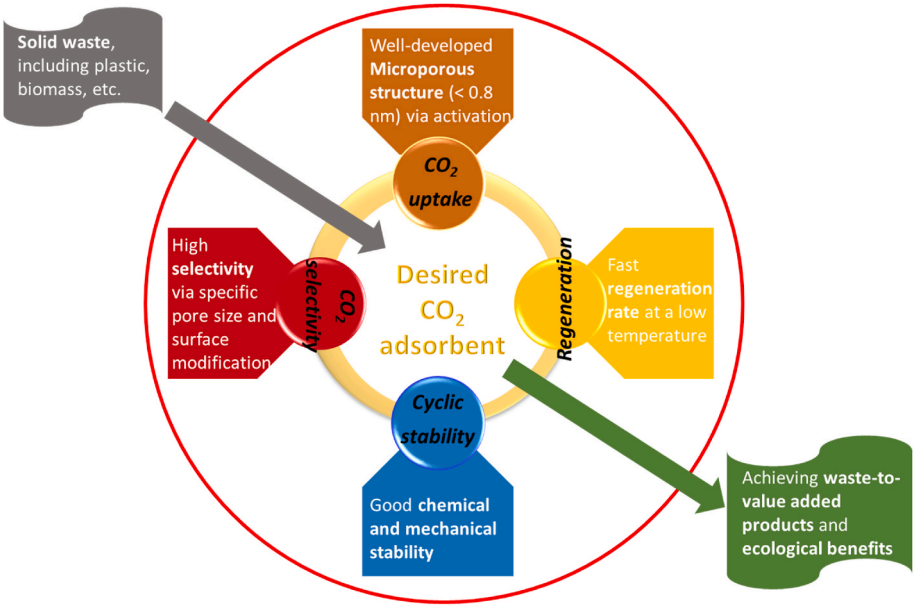

Fig. 4. Major criteria of the desired CO_2 adsorbents derived from solid waste.

Isotherms and dynamic CO_2 adsorption capacities are critical indicators for evaluating the CO_2 capture performance of the PCs. However, the applicability of CO_2 adsorbents in commercial cyclic processes cannot be directly inferred based on these parameters. Moreover, obtaining the quantity of CO_2 that can be sequestrated over a complete adsorption–desorption cycle is crucial [132]. Therefore, for PCs to be used in CO_2 capture units, the working capacity during a complete CO_2 adsorption–desorption cycle should be analyzed [132], and a detailed swing analysis of CO_2 capture using PC materials should be carefully performed. In swing analysis of PC-based CO_2 capture, the operating temperature and pressure are commonly considered as two key factors that significantly affect the working capacity.

The effect of the operating temperature on the working capacity of PCs with regard to CO_2 capture was studied. Zhang et al. [133] tested the CO_2 adsorption–desorption performance of PCs at ambient temperatures with desorption at higher temperatures and determined the working capacity of PCs for CO_2 capture. They further investigated CO_2 adsorption at a relatively high temperature, because flue gas is typically emitted from power plants post-combustion at approximately 75 °C. Mallesh et al. [134] analyzed the adsorption and desorption of CO_2 on waste *Entada rheedii* shell-derived PC at 70 °C and 140 °C, respectively, and reported that the working capacity of the PC was stable (4.4 mmol g^{-1}). These results indicate that SWDPCs can achieve satisfactory working capacities in different temperature ranges.

In addition to the operating temperature, the effect of the operating pressure on the working capacity has also been addressed. The pressure swing process is considered to be time-saving and plays a major role in evaluating the CO_2 capture performance of the PCs. Plaza et al. [135] upcycled spent coffee grounds into PC for CO_2 capture at a constant temperature of 50 °C and achieved a working capacity of 1.66 mmol g^{-1} using helium as the purging gas to reduce the CO_2 partial pressure. Overall, these observations indicate that the working capacity is a key parameter for screening robust CO_2 adsorbents and a performance indicator for swing analysis to preliminarily evaluate the CO_2 capture performance of certain SWDPCs.

3.2. CO_2 selectivity

The ideal adsorbed solution theory (IAST) method (Eq. (8)) is most widely used for calculating the selectivity of CO_2 over other gases, particularly N_2, in flue gas. An alternative is the Henry's law approach (Eq. (9)) [4]. To predict the adsorption behavior of binary mixtures using experimental IAST pure-gas isotherms, single-component isotherms should be first fitted using a suitable model. There are several models for isotherm fitting; however, the final choice highly depends on the mechanism of the specific adsorption behavior and the range of obtained experimental data. Adsorption isotherms are generally obtained at equilibrium, at a specific pressure and temperature. According to Eq. (9), the selectivity is calculated using Henry's constant (K_H) of the target gases. However, the ratio of *the* K_H values of the gases can only reflect the real selectivity of the mixture on the prepared PCs at very low pressures and low gas loadings. Because volumetric single-gas adsorption isotherms can be easily obtained, CO_2 selectivity over N_2 can be calculated using the IAST and Henry's law approaches without utilizing any special equipment for mixed-gas measurements.

$$S_{CO_2/N_2} = x_{CO_2}/x_{N_2} \cdot y_{CO_2}/y_{N_2} \tag{8}$$

$$S_{CO_2/N_2} = K_H\,(CO_2)\,/\,K_H(N_2) \tag{9}$$

A *PET6KU*$_{one\text{–}pot}$ sample with a CO_2 adsorption capacity of 4.58 mmol g^{-1} at 25 °C and 1 bar was used for CO_2 and N_2 adsorption, and the results are shown in Fig. 6a [66]. Using the pure-gas isotherms, the IAST CO_2 selectivity over N_2 for a 10%CO_2/90%N_2 flue gas was calculated as 18, 19, and 28 at 0 °C, 25 °C, and 50 °C, respectively. These values were similar to or higher than the selectivities of SWDPCs. In addition to the proper pore size, an effective functional group could enhance CO_2 selectivity by performing surface modification. The analysis of the N1s and O1s profiles of the PET-derived *N*-doped PCs in the full X-ray photoelectron spectroscopy (XPS) spectrum (Fig. 6b, c, and d, respectively) revealed that N and O functional groups were successfully introduced into the PC. The major peaks in the XPS profiles of the analyzed samples indicated the presence of different functional groups (i.e., –H, –OH, ether, and ester) in their structure. To elucidate the effects of the functional groups, a GCMC simulation was performed, and the major findings are shown in Fig. 5f [67]. The results suggest that the –OH functional groups enhance the interactions between the microporous carbon adsorbents and CO_2 gas molecules and effectively promote CO_2 selectivity over N_2 [66,92,136].

Liu et al. [128] prepared hierarchical ultramicro/mesoporous biocarbons from low-grade rice husks using a facile one-step method. The prepared samples exhibited high adsorption capacities of 1.84 mmol g^{-1} and a record-high CO_2/N_2 selectivity value (determined via Henry's

Table 3
Summary of solid porous carbons derived from plastic and biomass waste and their CO_2 capture performance. Here, S_{BET} and V_{total} denote the Brunauer–Emmett–Teller surface area and total pore volume, respectively.

Precursor	Carbonization temp. (°C)	Activation		Surface modification	Sample	S_{BET}	V_{total}	O/C ratio[a]	N/C ratio[a]	Isothermal CO_2 adsorption capacity		Dynamic CO_2 adsorption capacity	CO_2 selectivity over N_2 at 25 °C[b]
		T (°C)	Agent			$m^2 g^{-1}$	$cm^3 g^{-1}$	%		25 °C, 1 bar	25 °C, 0.15 bar	30 °C, 1 bar	
										mmol g^{-1}			
PET waste bottles [66,67, 92,93]	700	700	KOH	–	PET–3–700	1960	0.83	–	–	–	–	2.31	–
	600	700	KOH	–	PET–KOH–973	1812	0.98	(9.29)	0	4.42	1.10	3.31	14 (0.15)
	600	700	KOH	Urea	$PET6KN_{one-pot}$	1162	0.47	(24.11)	(4.14)	4.58	1.13	3.51	19 (0.10)
	600	900	CO_2	–	PET6-CO_2-9	1482	0.607	(13.08)		3.63	1.05	2.68	–
Packing peanuts [94,95]	600	850	KOH	–	CMS–K3	1354	0.55	(11.73)	(0.92)	4.07	1.02	3.48	15 (0.15)
	500	700	KOH	–	WDC–03	1283	0.69	–	–	4.24	0.99	–	–
Spent coffee ground [96, 97]	–	700	K_2CO_3	–	CG700–5	1476	0.61	0	1.82	4.54	1.30	3.29	14 (0.15)
	400	600	KOH	Melamine	KMHC	990	0.55	–	–	–	–	2.67[§]	–
Coca Cola® [98]	200	600	KOH	–	CMC–3	1405	0.80	(16.89)	(4.73)	5.22	1.40	–	–
CDs and DVDs [99]	500	700	KOH		C–KOH–4	2710	1.27	9.32	8.61	3.30	0.90	–	–
Bee pollen [89]	800	800	KOH	–	K1PDC1	937	0.40	(26.93)	(1.99)	3.38	1.18		15 (0.15)
Petroleum coke [100,101]	450	700	KOH	–	PC–2:1–700	1433	0.60	16.83	0.40	3.68	0.98	3.02	14 (0.15)
	500	700	KOH	–	C500–K	1470	0.60	–	–	4.17	1.34	–	16 (0.15)
70% wood chips and 30% chicken manure [102]	–	850	KOH	–	WCMK	1409	0.83	32.58	0.01	2.92	0.63	1.75	9 (0.15)
Persian ironwood [103]	500	300	H_3PO_4	$Cu(NO_3)_2{\cdot}3H_2O$	HP5/Cu3–1	1954	1.63	–	–	6.78 [ξ]	–	–	–
Banana stems [104]	700	–	–	–	Banana fiber–FD–700	1260	0.81	16.67	0	5.00	1.78	–	–
Sawdust [84,105,106]	400	700	KOH	–	ACSD–2700	1830	0.78	18.82	0	4.90	1.10	–	–
	–	600	$MgCl_2$	–	mPC–MgO–873	306	0.16	37.92	–	–	–	5.45 [β]	–
	250	600	KOH	–	SD2600P	1066	0.59	–	–	5.80	2.00	–	–
Coconut shell [107–111]	500	600	KOH	–	C-600–3	1172	0.44	–	–	4.23	1.31	–	–
	800	800	CO_2	–	Cnut–3.5 h	1327	0.65	–	–	3.90	1.19		
	500	600	K_2CO_3	Urea	CN–600–3	1082	0.39	–	3.13	4.70	1.23	–	11 (0.15)
	500	650	KOH	Urea	NC–650–3	1535	0.60	–	1.12	4.80	1.49	–	15 (0.10)
	500	650	KOH	Ammonia	NC–650–1	1483	0.66	–	6.51	4.26	1.28	–	–
Argan hard shell [112]	700	850	KOH	–	ARG–K–Im	1890	0.87	16.81	4.14	5.63	1.62	–	–
Hazelnut shell [60]	500	550	$NaNH_2$	–	HSC–550–1	1099	0.45	–	2.93	4.32	1.48	–	17 (0.10)
Walnut shell [113–115]	150 (H_3PO_4)	850	KOH	Urea	HAC–KOH–850	2354	1.26	29.80	1.14	3.08	0.64	–	–
	500	450	$NaNH_2$	–	NAC–450–2.5	1687	0.94	–	2.60	3.06	0.68	–	–
	600	600	KOH	Urea	KNWS–2–600–120	1315	0.65	–	–	7.42	–	–	–
Shrimp shell [116]	400	700	KOH	–	SA–1–700	1406	0.72	–	–	4.20	1.01	–	23 (0.15)
Water chestnut shell [69, 117]	500	500	$NaNH_2$	–	WSC–500–1	1416	0.58	–	3.13	4.50	1.32	–	23 (0.10)
	500	700	KOH	Melamine	ANCs–3–700	3401	2.50	–	–	4.70	1.97	–	21.5 (0.15)
Pigskin collagen [118]	–	600	$Ca(NO_3)_2$/ K_2CO_3	–	CPC–600	1165	1.03	35.94	16.07	4.40	1.83	–	–
Poplar catkins [119]	400	800	$ZnCl_2$	–	NHPCT–4–8	1455	0.68	8.64 (7.20)	2.41 (1.71)	4.05	0.92	–	–
Pineapple waste [120]	210	700	$K_2C_2O_4$	–	C–K–700	1076	0.08	–	0.38	4.25	1.31	4.22	–
Garlic peel [121]	400	600	KOH	–	AC–26	947	0.51	–	–	4.22	1.21	–	–
Fallen leaves [122]	600	700	KOH	–	LC2–700	1600	0.65	–	1.54	4.41	1.55	–	–
Sugarcane bagasse [123]	600	600	KOH	Urea	UC–15–2–600	1113	0.57	–	2.37	4.80	1.54	4.76	–
Rotten strawberries [124]	180	650	KOH	–	SC–650–2	1117	0.52	–	6.90	4.49	1.48	–	20 (0.10)
Jujun grass [125]	250	700	KOH	–	ACGR2700	1512	0.74	–	–	4.90	1.50	–	–
Camellia japonica [125]	250	700	KOH	–	ACCA2700	1353	0.67	–	–	5.00	1.50	–	–
Gelatin and starch [126]	450	700	KOH	–	GSK1–700	1636	0.51	29.58 (30.17)	4.20 (4.30)	3.84	0.88	–	–
Rice husk [127,128]	520	710	KOH	–	PC1–710	1041	0.53	–	–	4.16	1.55	–	–
	200	700	KOH	PEI	R7–2 T–10PEI	1190	0.78	–	–	4.50	1.90	–	–
Pinecone [129]	600	700	KOH	–	PC2–700	1680	0.61	17.99	0.60	4.75	1.50	–	–
hickory chips [130]	450	600	$FeCl_3{\cdot}6H_2O$	–	FeHC(0.1)	–	–	–	–	–	–	1.18	–

The numbers in parentheses are the partial pressures of CO_2; [§] at 35 °C; [β]at 80 °C; [ξ] at 30 °C and 1 bar.
[a] Obtained via elemental and X-ray photoelectron spectroscopy analysis.
[b] Calculated using ideal adsorbed solution theory selectivity.

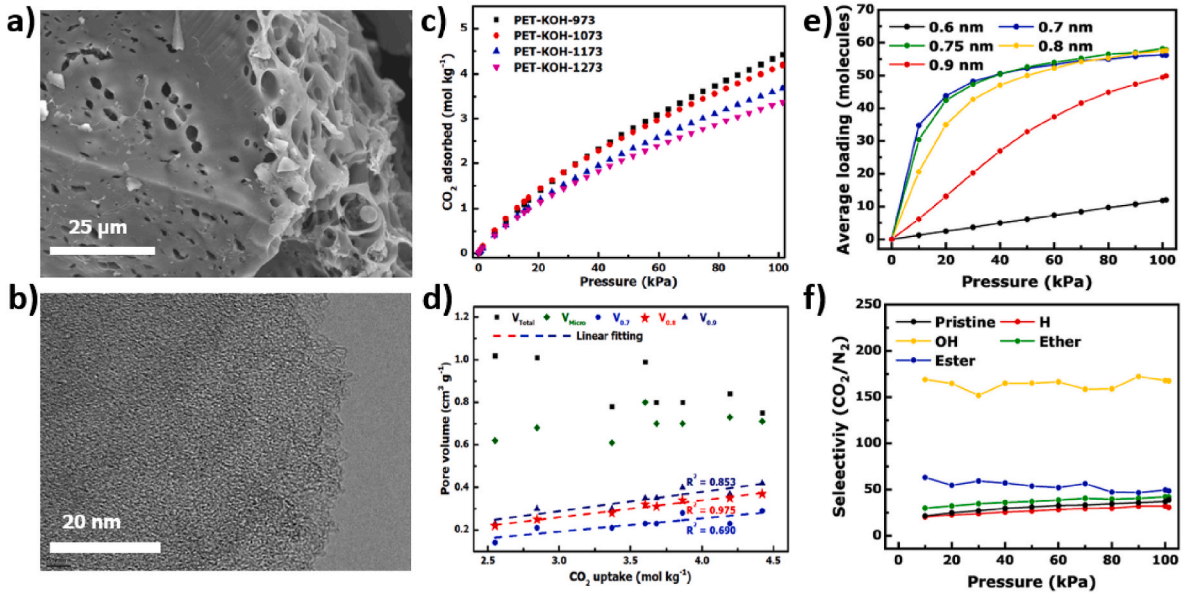

Fig. 5. a) Scanning electron micrograph (SEM) and b) transmission electron micrograph (TEM) of potassium hydroxide (KOH)-activated polyethylene terephthalate (PET–KOH–973). c) CO_2 adsorption isotherms of PET–KOH–x at 25 °C, d) CO_2 uptake dependence on pore volume at 25 °C and 1 bar, e) CO_2 adsorption isotherms of pristine bilayer graphene with 0.6, 0.7, 0.75, 0.8, and 0.9 nm pores, and f) CO_2 selectivity over N_2 in a 0.7 nm pore CO_2–N_2 (15%/85%) binary mixture system [67]. Here, $V_{0.7}$, $V_{0.8}$, and $V_{0.9}$ are the cumulative pore volumes limited by narrow micropores smaller than 0.7, 0.8, and 0.9 nm, respectively.

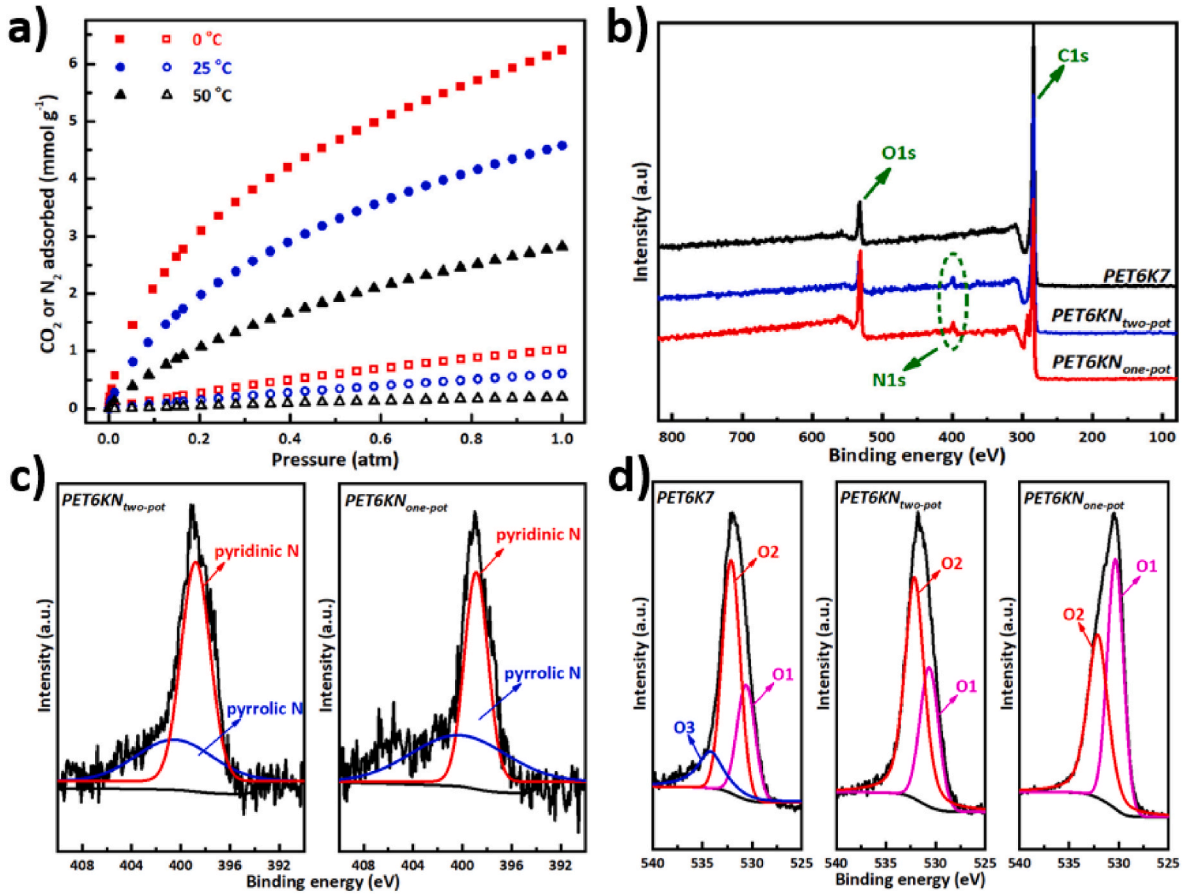

Fig. 6. a) CO_2 and N_2 adsorption isotherms on *N*-doped polyethylene terephthalate (*PET6KN*$_{one-pot}$) at three temperatures (the solid and open symbols represent CO_2 and N_2 adsorption data points, respectively). High-resolution X-ray photoelectron spectroscopy: b) full survey, c) N1s, and d) O1s profiles of the prepared samples [66].

law) of up to 212 at 25 °C and 0.15 bar. This was primarily ascribed to the unique combination of high ultramicropore volumes, narrow pore-size distribution, and modified surface functional groups by the enhanced K intercalation as a result of the applied compaction.

For CO_2 gas separation, the breakthrough data obtained using fixed-bed reactors can predict CO_2 selectivity more accurately than Henry's law [4,137] because breakthrough studies are typically performed under kinetic flow conditions and non-equilibrium settings. Kaur et al. [137] performed a breakthrough CO_2 adsorption study on waste PET plastic-derived nanoporous carbon. The breakthrough curves of the prepared samples are shown in Fig. 7a. The scanning electron micrographs (SEMs) of the prepared samples (i.e., Act–3–700 (Fig. 7b)) revealed a well-developed pore structure. Moreover, Act–3–700 (BET surface area of 1690 $m^2\ g^{-1}$ and micropore volume of 0.78 $cm^3\ g^{-1}$) exhibited the highest CO_2 adsorption capacity of 1.31 mmol g^{-1} at 30 °C and a CO_2 concentration of 12.5%. The CO_2 uptake of Act–3–700 changed significantly with the temperature and CO_2 concentration of the target gases (Fig. 7c), most likely because physisorption was the predominant mechanism during the CO_2 capture process. The breakthrough curves of CO_2/N_2 at 30 °C and a CO_2 concentration of 12.5% are shown in Fig. 7d. A hump in the breakthrough curve of N_2 was observed at $C/C_0 > 1$. This high N_2 occupancy of vacant sites during the initial stage was due to the concentration of N_2 being higher than that of CO_2. However, over time, N_2 was replaced with CO_2, which confirmed that Act–3–700 exhibited greater CO_2 selectivity over N_2.

3.3. Long-term stability

Considering CO_2 capture for practical applications, typical adsorption–desorption cyclic operations are essential. Specific technologies such as temperature swing adsorption (TSA), pressure swing adsorption (PSA), and electricity swing adsorption (ESA) can be deployed. However, appropriate solutions should be screened, tested, and optimized to obtain the optimal performance of the CO_2 adsorption–desorption process using PCs to maximize the working capacities. Thus, comprehensively evaluating the cyclic performance of PC materials is necessary.

While the working capacity is considered during swing analysis, cyclic performance is typically evaluated via cycle analysis, which is discussed in this section. Practical regeneration techniques include PSA (desorption at low pressure), vacuum swing adsorption (VSA desorption using vacuum), and TSA (desorption at high temperature) [138]. TSA cycles are a promising and practical approach for post-combustion CO_2 capture because PCs exhibit excellent CO_2 adsorption capacity under ambient conditions, physisorption dominates CO_2 capture on SWDPCs, and the energy required for CO_2 capture can be significantly decreased by avoiding compression or using vacuum for the large volumes of low-pressure gaseous streams required for PSA/VSA [132,139].

Appropriate performance indicators are required for generalized comparisons between different cycle configurations. Typical performance indicators, including purity, recovery, and productivity, are widely applied to evaluate the cyclic performance of solid waste-derived CO_2 adsorbents. Karimi et al. [140] synthesized PC for CO_2 capture from

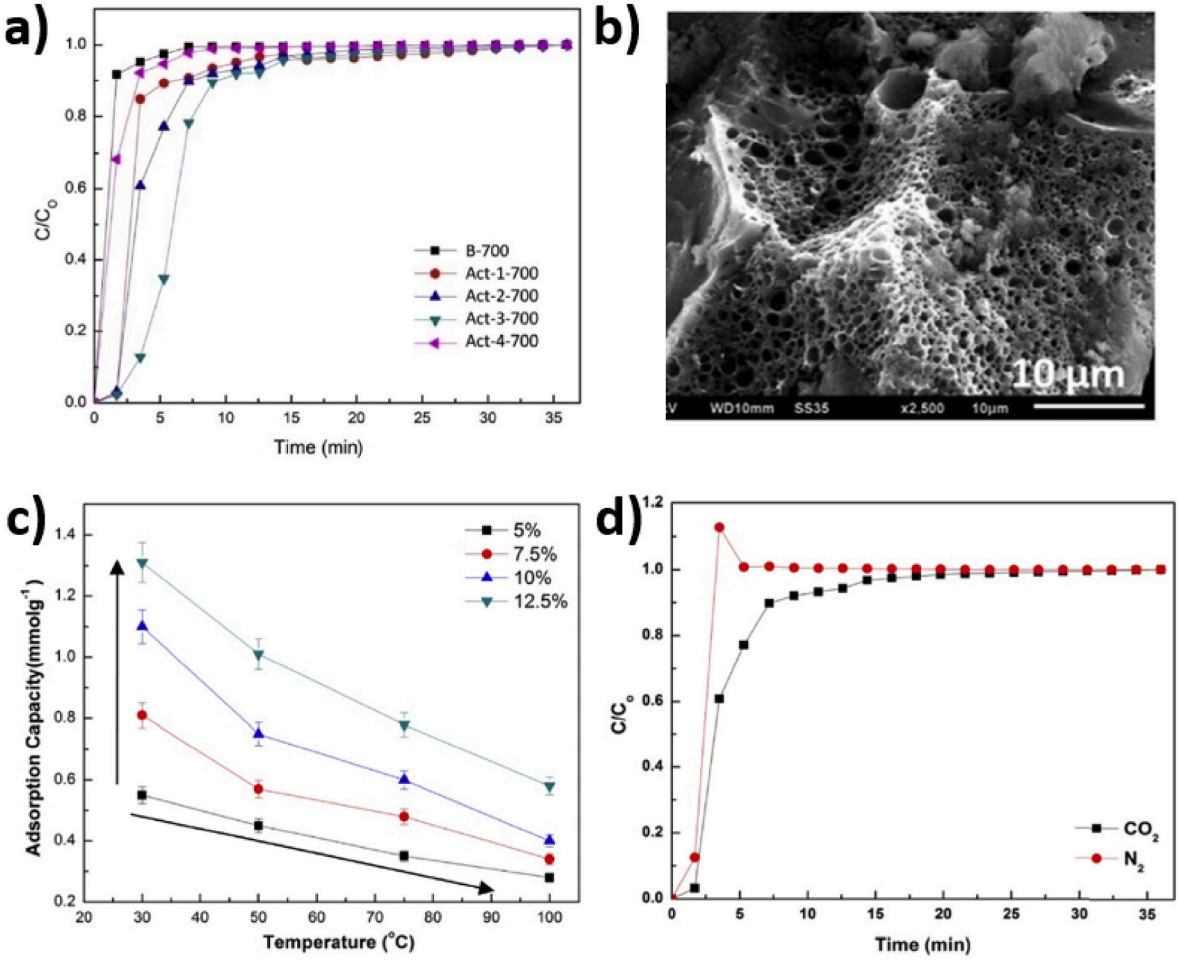

Fig. 7. a) Breakthrough curves of the prepared adsorbents, b) Scanning electron micrograph (SEM) of Act–3–700, c) Changes in the CO_2 adsorption capacity of Act–3–700 with the adsorption temperature and CO_2 concentration, and d) Selectivity of CO_2/N_2 on Act–3–700 for 12.5% CO_2 at 30 °C. Act–3–700 sample was obtained at an activation temperature of 700 °C with KOH to carbon mass ratio of 3. Reproduced with permission from Ref. [137].

MSW and evaluated the cyclic performance of the prepared samples in an in-house PSA unit with a stable working capacity of 2.6 mmol g^{-1} at 40 °C. Horstmeier et al. [141] numerically simulated a typical VSA cycle using functionalized PC; purity, recovery, productivity, and electric power requirements were considered to evaluate the cyclic performance of the prepared samples. Bahamon et al. [142] used date seed-derived PCs for their numerical simulation and calculated performance parameters, including the working capacity, purity, and energy requirement for regeneration, to optimize the cycle configuration and comprehensively compare the basic TSA, PSA, and VSA configurations. This study can be considered as a preliminary investigation of the cyclic performance of CO_2 adsorbents derived from solid waste. Hybrid regeneration techniques have also been proposed for this purpose. Plaza et al. [143] developed a PC-based vacuum/temperature/concentration swing adsorption (VTCSA) process for an olive stone-derived CO_2 adsorbent and used the specific energy penalty of avoided CO_2 (SEPAC) as a cyclic performance indicator. The application potential of the prepared CO_2 adsorbent was evaluated from the viewpoint of cyclic energy consumption. The key advantage of the VTCSA process is its low specific heat duty, which can be achieved using waste heat.

In summary, the practical application potential of SWDPCs should be evaluated considering their cyclic performance based on performance and energy consumption-related indicators. Owing to the lack of unified energy consumption calculations, a consistent energy efficiency assessment is still lacking, and this aspect needs to be explored in the future.

3.4. Other parameters

In addition to the factors mentioned above, the cost-effectiveness, isosteric Q_{st}, and moisture tolerance of adsorbents should be thoroughly investigated. Cost-effectiveness is an inherent advantage when upcycling solid waste into CO_2 adsorbents. Q_{st} is an indicator of the strength of the interactions between PCs and CO_2 molecules, and its value depends on the PC configuration. A high Q_{st} value indicates high energy consumption for the regeneration of the CO_2 adsorbent. Typically, the Q_{st} values of PCs range between 20 kJ mol^{-1} and 30 kJ mol^{-1}; the values can be higher if the PCs are doped with effective functional groups [66,67,87]. In addition, high moisture tolerance is considered an essential parameter for evaluating the performance of CO_2 adsorbents. Moisture significantly affects the CO_2 adsorption performance of the PCs and decreases their CO_2 uptake and CO_2 selectivity. As a typical case study, the flue gas from a coal-fired power plant was emitted post-combustion at a temperature of approximately 75 °C and a CO_2 partial pressure of approximately 0.15 bar accompanied by moisture. Zhao et al. [144] proposed a CO_2/H_2O competitive adsorption model from the perspective of thermodynamics, emphasizing that the adsorption entropies and enthalpies were temperature-dependent and would switch the relative order of Gibbs free adsorption energy between adsorbed CO_2 and H_2O. Zhao et al. [145] proposed a thermodynamic molecular pump (TMP) to quantitatively resolve the contradictions between the promotion and impedance of CO_2 adsorption by H_2O. This TMP-guided evaluation demonstrated that the Gibbs free adsorption energy of H_2O is a key indicator of the CO_2 adsorption performance owing to its contribution to the total driving energy, providing useful guidance for effectively screening CO_2 adsorbents considering the co-existing H_2O.

4. Machine learning for the optimization of the synthesis of solid waste-derived porous carbons

Traditionally, the screening and synthesis of PCs rely on the knowledge and intuition of researchers to generate a library of promising candidates, followed by experimental screening using a trial-and-error approach, also known as the direct approach [146]. An alternative to the direct approach is *in silico* screening using *ab initio* methods, which involves molecular simulation of promising compounds with target properties. However, considering the complexity of the system, these approaches present significant limitations, as dynamic and molecular interactions are very demanding in terms of computational power and duration [147,148]. Therefore, recent developments in the field of artificial intelligence, specifically applied ML and deep learning (DL), as well as more widely available and less expensive graphic processing units and parallel computing [149,150], are promising methods for integrating the direct approach and *in silico* method to accelerate the discovery and elucidate the reaction mechanisms of target-specific PCs.

Most studies on the application of ML for the analysis of PCs have focused on developing forward models (i.e., prediction of target features) based on a set of input features and on establishing model validity by achieving suitable or acceptable accuracy levels [146]. This has typically been followed by feature analysis, wherein the input features with the highest effect on the target variable, as determined by the forward model, are deduced using the Pearson correlation matrix, Shapley values, or related methods [146,151]. Subsequently, these data are corroborated with expert knowledge to draw conclusions from the model's findings. To date, a few ML studies have suitably predicted the CO_2 adsorption capacities of PCs based on their structural and textural properties and determined the relationships between the CO_2 adsorption capacity (using the characteristics of PCs) and corresponding adsorption conditions, even for nonlinear interpolation.

Zhu et al. [152] modeled the CO_2 adsorption behavior of 155 PCs using ML and developed a mapping function for the isothermal CO_2 adsorption capacities of these carbon materials based on a set of 10 input features categorized into textural properties, chemical composition, and adsorption pressure. A tuned random forest algorithm exhibited a good prediction ability ($R^2 > 0.9$) for the CO_2 adsorption capacity of the analyzed PCs. Subsequent feature analysis revealed that the textural properties of the PCs had a greater effect on the CO_2 adsorption capacity than their chemical composition. Specifically, the mesopore and micropore volumes of the PCs had significant effects on the CO_2 adsorption capacity at low pressure (0.1 bar), and ultramicropores contributed the most at higher pressures (> 0.6 bar). Owing to the complexity of the analysis, the effect of chemical composition was not completely elucidated. However, the authors claimed that the N content of the PCs was positively correlated with their CO_2 adsorption capacity.

Wang et al. [153] developed a deep neural network (DNN) framework for the CO_2 and N_2 uptake of PCs based on experimentally determined textural properties such as micropore volume, mesopore volume, and Brunauer–Emmett–Teller (BET) surface area. Their DNN model was used to screen high-performance PCs with high CO_2 and low N_2 uptakes. The analytical inference of their model revealed that the highest CO_2/N_2 selectivity was achieved at the lowest N_2 uptake. Low N_2 uptake was attributed to the disruption of N_2 adsorption by the mesopores. In addition, Wang et al. [154] used a convolution neural network to establish a mapping function between the porosity and gas-separation performance of PCs. In an unconventional yet novel approach, a one-dimensional image of an N_2 isotherm at −196 °C (which is representative of the pressure points and corresponding adsorbed volumes) was fed into five-layered convolutional networks to extract information on the porosity of PCs. The extracted information, temperature (0–50 °C), and pressure (0–1 bar) were fed into three fully connected input layers and one regression layer to an output neuron, which predicted the gas-separation performance of PCs using CO_2/N_2 as a case study. The model revealed that PCs with a bimodal pore-size distribution of well-separated mesopores (3–7 nm) and micropores (< 2 nm) exhibited the most promising CO_2/N_2 selectivity.

More recently (Fig. 8), Yuan et al. [42] presented a systematic study to show how the concepts of ML can be applied for predictive analytics and shed valuable insights into CO_2 adsorption using PC-derived biomass waste. The authors reviewed 76 peer-reviewed publications and created a set of 527 data points using the data-imputation method. They devised ML models to predict biomass waste-based CO_2 adsorption as a function of their textural properties, compositional properties, and

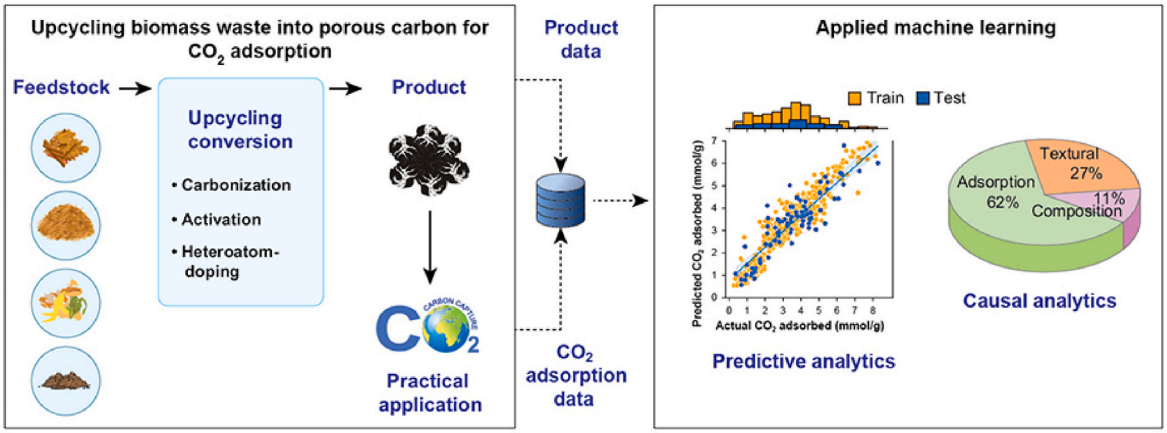

Fig. 8. Schematic of applied machine learning (ML) techniques for the prediction of CO_2 adsorption on biomass waste-derived porous carbons [42].

adsorption parameters of the CO_2 capture process. They primarily developed tree-based ML models, including gradient boosting decision trees (GBDT), extreme gradient boosting (XGB), and light gradient boost (LGB), where the GBDT had the best predictive performance with R^2 of 0.98 and 0.84 on the training and test data. They further classified the dataset into regular PCs and heteroatom-doped PCs; again, the GBDT model exhibited the best predictive performance. They also evaluated the significant features using local sensitivity analysis tools, including mean decrease in accuracy (MDA) and partial dependence plots (PDP), and concluded that adsorption parameters were most critical to the CO_2 adsorption process, followed by textural and compositional properties.

Considering the lack of studies on the use of ML- and DL-based analyses of SWDPCs, research in this domain is still in its infancy. However, further inspiration can be drawn from related studies on the use of

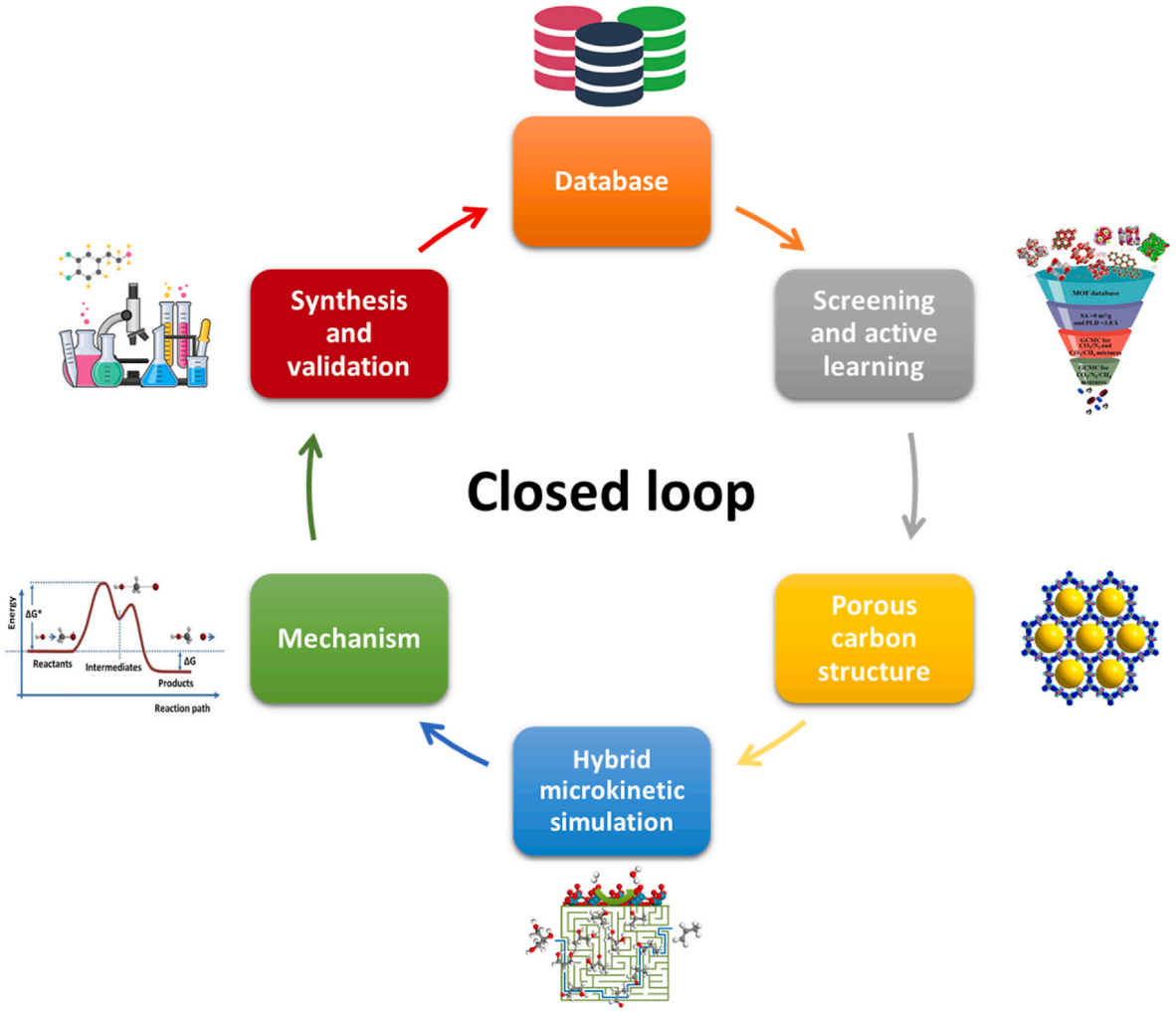

Fig. 9. Closed-loop guideline integrating the artificial intelligence (AI) methodologies, specifically smart data-machine intelligence-automated synthesis for solid waste-derived porous carbons (SWDPCs).

zeolites, metal–organic frameworks (MOFs), and covalent organic frameworks (COFs) for CO_2 capture and conversion, wherein ML concepts have been adopted and applied. Some notable studies include the use of advanced ML algorithms to rapidly and accurately recognize high-performance MOF materials for CO_2 capture [150,155], employment of a self-tuning automated ML architecture to predict the adsorption capacities of MOFs with few experimental data points (< 100) [156], accelerated discovery of zeolites [157], prediction of the mechanical properties of zeolites based on their geometry [158], and use of a more generic ML framework for large-scale screening of potential MOFs for gas adsorption capacities [147].

Owing to their advantages such as intuitiveness, high computational prowess, and wide acceptance and application across scientific disciplines, ML techniques are likely to draw increasing interest in

Table 4
Summary of the life-cycle analysis studies on solid waste-derived CO_2 adsorbents.

Raw material	Product	Functional unit	System boundary	Impact categories*	Impact assessment	Database	Software
Coconut shell [164]	PC	1 tonne PC produced	Cradle–to–grave	1–9	Midpoint	Ecoinvent v3.0	GaBi 6.0
Exhausted olive–waste cakes [165]	PC	1 kg PC produced	Gate–to–gate	1–10	Midpoint	Ecoinvent v2.2	Simapro 7.3
Corn pericarp [166]	PC	1 kg PC produced	Gate–to–gate	a–d, f, i	Endpoint	Ecoinvent v3.1	Simapro 8.0
Woody biomass [167]	PC	1 kg PC produced	Cradle–to–gate	1–3, 5, 7, 11–14,16	Midpoint	N.A.	Simapro 8.0
Forest residues [168]	Biochar	1 tonne marketable biochar; 1 tonne forest residue	Cradle–to–gate	5	Midpoint	N.A.	SimaPro 8.5
Eucalyptus waste [169]	PC	1 kg PC produced	Cradle–to–gate	1–9,15	Midpoint	Ecoinvent 3.4	SimaPro 8.2
Agricultural residues, yard waste and switchgrass energy corps [170]	Biochar	1 tonne dry biomass	Cradle–to–grave	5, 10	Midpoint	N.A.	Microsoft Excel
Pine sawdust [171]	Biochar	1 tonne biochar produced	Gate–to–gate	1–9,15	Midpoint	European life-cycle database	OpenLCA
Forest harvest residue, sawmill residue and underutilized trees [172]	PC**	1 GJ energy for propelling an aircraft engine	Cradle–to–grave	2, 3, 5, 11–14, 16	Midpoint	Ecoinvent	GREET*** and Simapro 8.1
Woody biomass processed into wood pellet [173]	Biochar	1 tonne biochar produced	Cradle–to–grave	2, 3, 5, 7, 9, 12–15, 17–20	Midpoint	Ecoinvent and USLCI	Simapro 8.1
Woody shrub or agricultural residue [174]	Biochar	Preparation and sequestration of 1 kg biochar	Cradle–to–grave	a–h, i	Endpoint	Ecoinvent 3.2	N.A.
Soybean shells [175]	PC	1 kg PC produced	Cradle–to–gate	5, a–d, i	Endpoint	Ecoinvent 3.1	SimaPro 8.0
Corn fodder and forest residues [176]	Biochar	1 tonne dry biomass	Cradle–to–grave	5	Mid–point	N.A.	Microsoft Excel
Agriculture residue [177]	Biochar	1 tonne maize produced per year	Cradle–to–grave	a–d, f, i	Endpoint	Ecoinvent 2.2	N.A.
Ten types of agriculture residue available in UK [178]	Biochar**	1 tonne dry feedstock, 1 tonne biochar produced, 1 MWh electricity produced, 1 ha (10 000 m^2) land used to produce the feedstock	Cradle–to–grave	5	Midpoint	N.A.	N.A.
Sargassum–Horneri [179]	PC	1 kg PC produced	Cradle–to–gate	5	Midpoint	N.A.	N.A.
Pig mature and willow woodchips [180]	Biochar	1 tone of biochar	Cradle–to–grave	2-4,7,9,12–14,18-21,24	Midpoint	Ecoinvent 3; ELCD; USLCI	SimaPro 8.3
Sugarcane [181]	Biochar**	1 ha of sugarcane crop for São Paulo state, 1 tonne of CO_2 eq sequestered.	Cradle–to–grave	5	Midpoint	EcoInvent 3.6	SimaPro 9
Wood waste [182]	Biochar**	1 year of operation of the pyrolysis plant (800 kg h^{-1} dry wood, 1250 t yr^{-1} biochar)	Cradle–to–grave	2,3,5,7,8,14,17–20,24	Midpoint	EcoInvent 3.6	Brightway2
Perennial grass (Miscanthus) [183]	Biochar	1 tone of biochar	Cradle–to–gate	2,3,5,7,11,12–14,16,18	Midpoint	/	SimaPro
Cattle manure [184]	Biochar	1 kg of biochar	Cradle–to–grave	1–9	Midpoint	AGRIBALYSE and OpenLCA database	OpenLCA
Polyethylene terephthalate waste bottle [163]	PC	1 kg PC produced, used and disposed	Cradle–to–grave	1–8, 21–23	Midpoint	CLCD–China–ECER–0.8 Ecoinvent 3.1 ELCD 3.0	eFootprint

*Midpoint impact categories: [1]Abiotic depletion, [2]Acidification potential, [3]Eutrophication, [4]Freshwater aquatic ecotoxicity, [5]Global warming potential, [6]Human toxicity potential, [7]Ozone layer depletion, [8]Photochemical ozone creation potential, [9]Terrestrial ecotoxicity, [10]Cumulative primary energy demand, [11]Smog, [12]Carcinogenics, [13]Non–carcinogenics, [14]Respiratory effects, [15]Marine aquatic ecotoxicity, [16]Ecotoxicity, [17]Mineral extraction, [18]Non-renewable energy, [19]Terrestrial acidification, [20]Ionizing radiations, [21]Primary energy demand, [22]Water resource depletion, [23]Particulate matter, and [24] Land occupation.
*Endpoint impact categories: [a]Fossil depletion, [b]Ecosystem climate change, [c]Particulate matter formation, [d]Human health and climate change, [e]Land transformation and occupation, [f]Metal depletion, [g]Ozone depletion, [h]Human toxicity, [i]Other.
**PC is produced as a byproduct.
***Greenhouse Gases Regulated Emissions and Energy use in Transportation (GREET) software.

comprehensive investigations pertaining to SWDPCs. Herein, we present certain guidelines for enabling AI-related technologies to foster the accelerated screening, design, and synthesis of SWDPCs via closed-loop life-cycles (Fig. 9).

Although experimental studies on SWDPCs for gas separation and storage have been prevalent for almost a decade, few dedicated or structured databases have listed the details of all experimentally synthesized PCs and their specific physicochemical properties. Therefore, a curated comprehensive database is proposed. Text mining using natural language processing and associated ML techniques can facilitate searching the vast literature that contains unstructured data on intrinsic (i.e., crystallinity, pore size, binding energies, hydrophobicity) and extrinsic (i.e., feedstock composition and concentration, activating agents pH, and reaction temperature) synthesis parameters of SWDPCs and can curate them into a structured format, as recently achieved in the field of material science [159,160].

Once such curated databases are developed, ML-based forward models can be devised for screening targeted high-performance SWDPCs or predicting their performance under a given set of conditions, as discussed in Section 2. Furthermore, active learning frameworks, using approaches such as Bayesian optimization, which continuously learn and adapt as they explore the already curated chemical space, can expand the development of molecular entities of SWDPCs in regions of high uncertainty, thereby enabling the discovery of regions of molecular space with desirable properties under different physical conditions [146,149]. This combined approach (i.e., using active learning frameworks in conjunction with ML techniques) could address the challenging endeavor of screening and expediting the guided synthesis of high-performance SWDPCs, which depend on various intrinsic and extrinsic parameters and have been rendered infeasible and nonpractical via the direct approach.

A gradual extension of the aforementioned methods and concepts, which are more intuitive and definitive than the conventional trial-and-error approach, would enable guided experiments for synthesizing high-performance SWDPCs with the desired properties. Additionally, the guided synthesis procedures can be subjected to active learning approaches (which can guide the cycles of experiments from a few sample points to iterative extensions) and looped with online automated synthesis platforms [161,162] to develop the concept of chemical robotics for the efficient, direct, and accelerated synthesis of PCs with desired properties.

5. Life-cycle assessment of CO_2 capture technology based on solid waste-derived porous carbons

The evaluation of the environmental performance of SWDPCs and biochar has attracted increasing interest since 2010. Table 4 presents an overview of life-cycle assessment (LCA) studies, summarizing the functional units (FUs), system boundaries, impact categories, impact assessment methods, databases, and software used in the pertinent studies. Although different types of solid waste can be used as precursors for CO_2 adsorbents, existing studies have primarily focused on PC or biomass waste-derived biochar using different raw materials. Wang et al. [163] were the first to explore the life-cycle performance of waste PET plastic-derived PC for CO_2 capture and its potential to achieve negative CO_2 emissions.

5.1. Functional unit and system boundary

The goal and scope definition of LCA studies include three main elements: specifying the aim of the study, defining the functional unit, and the corresponding system boundaries. Typically, LCA studies on PC or biochar aim to quantify the potential environmental impacts of associated production processes. The goals of the reviewed LCA studies can be subdivided into four categories: single scenario, scenario comparison, factor comparison, and optimization. Three of the reviewed studies comparatively assessed different waste management methods or PC/biochar production methods: Heidari et al. [169] evaluated the environmental impacts of using eucalyptus wood for bioenergy and PC production; Pierobon et al. [172] performed an LCA of woody biomass-based bio-jet fuel with PC and lignosulfonate as coproducts and compared their prepared fuel with petroleum-based jet fuel; and Nie et al. [185] performed an LCA of transportation biofuels from hydrothermal liquefaction of forest residues. Bergman et al. [167] compared the environmental impacts of syngas-to-electricity and biochar-to-PC production from woody biomass as well as from natural gas and coal (commercially available alternatives). Numerous studies have been conducted to investigate the environmental performance of waste-to-PC/biochar systems in terms of specific factors, which mainly include pyrolysis methods [169,174,178], biochar production systems [168,177,184], types and quality of feedstocks [168,170,180,181], on-site or off-site biochar utilization [182], and allocation methods [172]. In addition, using LCA results as an environmental indicator, Loya-Gonzalez et al. [166] optimized the production process of PC from corn pericarps.

The FU is a reference parameter for quantifying the performance of production systems and plays an important role in comparing different products/processes. As mentioned by Roberts et al. [170], in addition to PC/biochar production, the biomass waste-to-PC/biochar process can involve several associated processes such as biomass waste management, carbon sequestration, energy generation, and soil amendment. Therefore, the selection of FU for LCA highly depends on the aim and scope of the study. In the reviewed studies, the most widely used FU is the production output, such as the mass of PC/biochar (i.e., 1 kg tonne^{-1} of PC/biochar produced). In several studies, FU has been defined as the mass of waste input (i.e., 1 tonne of processed waste biomass). Three studies defined more than one FU to elucidate the LCA results. For example, Puettmann et al. [168] used three FUs, including 1 tonne of marketable biochar, percentage of fixed C in the biochar, and 1 dry tonne of forest residue. Similarly, Hammond et al. [178] expressed LCA results using various metrics, such as 1 dry tonne feedstock, 1 tonne biochar produced, 1 MWh electricity produced, and 1 ha land used to produce the feedstock. Moreover, Pierobon et al. [172] used 1 GJ of energy as the FU for propelling an air engine because PC is the co-product of the biomass-based bio-jet fuel production process. Sparrevik et al. [177] selected 1 tonne maize per year as the FU because their study was conducted from an agricultural perspective and included both biochar production and soil amendment.

A typical LCA system boundary for different solid waste feedstocks used for PC production is shown in Fig. 10. Typically, the life-cycle process can be divided into three stages: raw material preparation, PC/biochar production, and PC/biochar application. Because PC/biochar production is the core of LCA studies, most reviewed studies have comprehensively analyzed this stage. Specifically, three production pathways were commonly mentioned in the reviewed studies; these included two PC production approaches and one biochar production approach. Not all the literature reviewed herein included the raw material preparation process (i.e., biomass/plastic production, collection, and transportation) in the LCA. Moreover, only four of the reviewed studies considered biomass production processes [168,175,180,183]. Another notable aspect of LCA studies is the extension of PC/biochar applications. Because of their well-developed porosity and stable C-rich content, PC and biochar can be used as soil amendments and for long-term carbon sequestration [177,182,173]. Therefore, several studies have investigated the soil application phases of PC/biochar products. Robbers et al. [170] considered the positive effects of improving fertilizer efficiency and reducing nitrous oxide (N_2O) emissions when biochar was used as a soil amendment.

5.2. Global warming potential and other environmental impacts

The results obtained using the midpoint method and the FU of 1 kg of

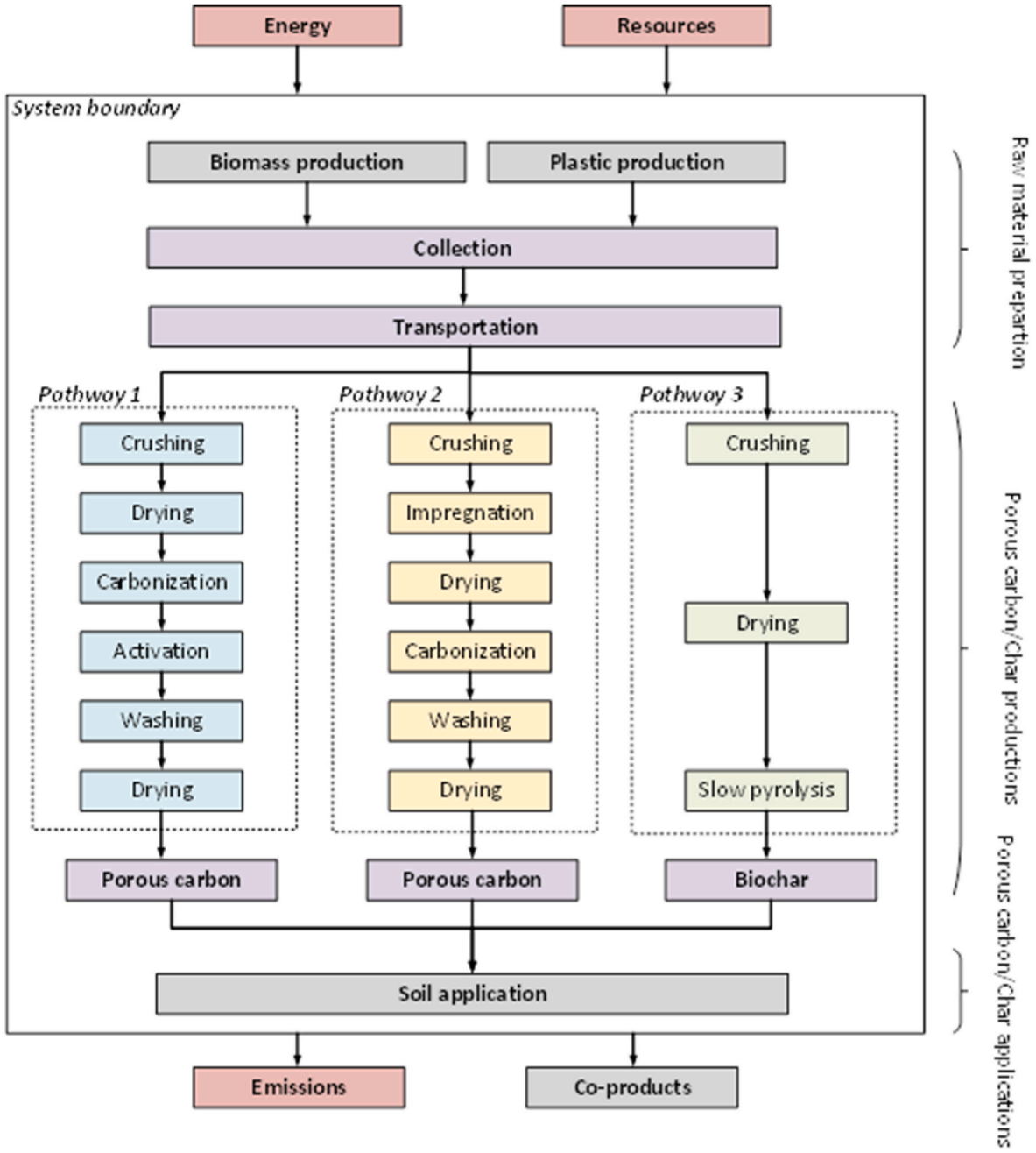

Fig. 10. Typical system boundary for solid waste-to-porous carbon/biochar life-cycle assessment.

PC/biochar produced (1 tonne was converted to 1 kg) are compared in this section. The representative global warming potential (GWP) of the three production process pathways (Fig. 10) is shown in Fig. 11 (with supplementary information in Table 5). For a fair comparison, all presented data were processed and presented with consistent functional units and comparable system boundaries. PC products have a relatively high GWP owing to their complex production processes. The GWP of biomass waste-derived PC was in the range of 5.5–11.1 kg CO_{2-eq}/kg PC, excluding the CO_2 absorbed during the biomass growth and soil application processes. The emissions of PET-derived PC were relatively higher (but < 14.0 kg CO_{2-eq}/kg PC) when greenhouse gas emissions during the PET production phase were included [163]. Puettmann et al. [168] evaluated the GWP impacts of biochar using the portable systems developed by Biochar Solutions Inc. (Lafayette, US) and revealed that the GWP of biochar produced from different forest residues ranged between 0.2 CO_{2-eq}/kg biochar and 1.0 CO_{2-eq}/kg biochar. In addition, a high GWP of 4.1 kg CO_{2-eq}/kg biochar produced from organic waste (primarily pine sawdust) was obtained in the study by Hersh and Mirkouei [171]. These four studies also considered atmospheric carbon sequestration during biomass growth [163,168,183,171]. The overall results indicated that when the system boundary was expanded to include biomass production and soil application stages, a negative GWP could be achieved for biomass waste-to-PC/biochar systems.

In addition to GWP, the negative impacts of cumulative energy demand (CED) and fossil fuel depletion potential have been addressed in several studies. The reported CED for PC production ranged between 118 and 167 MJ kg^{-1} of PC produced [169,167,165], and CED was the main contributor to fossil depletion potential. Arebn et al. [164] concluded that attention should be paid to freshwater aquatic and terrestrial ecotoxicity impacts owing to the wastewater generated during the carbonization process. Heidari et al. [169] indicated that terrestrial acidification and marine aquatic ecotoxicity had the greatest

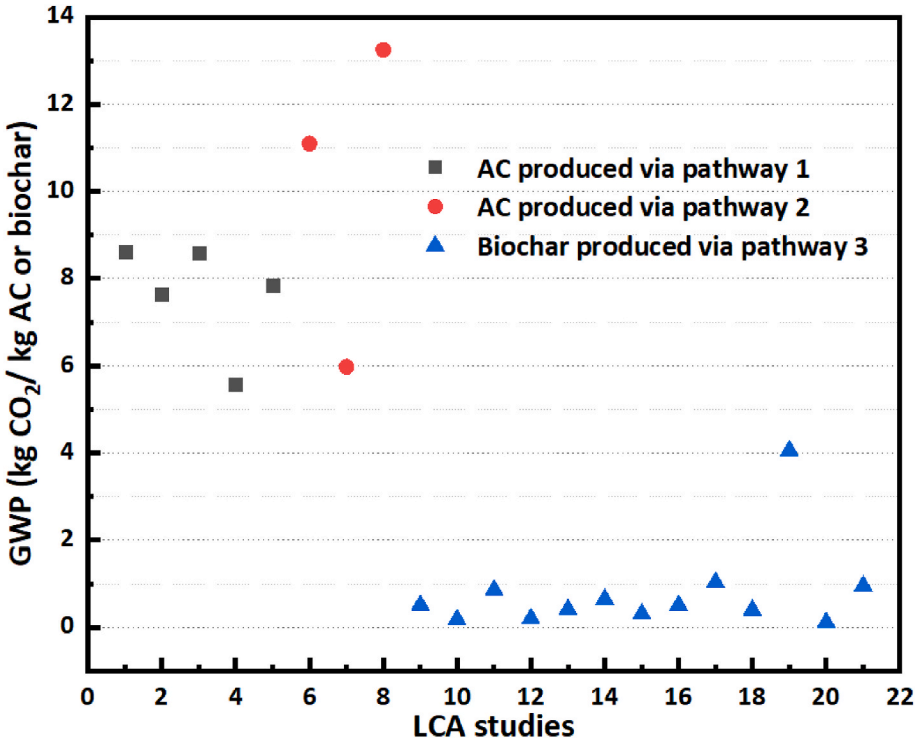

Fig. 11. Global warming potential (GWP) obtained from different life-cycle assessment (LCA) studies based on the functional unit (FU) of 1 kg porous carbon (PC)/ biochar produced [163,169,167,168,171,165,183,184,179].

Table 5
Supplementary information for Fig. 11.

Point No.	Precursors	Ref.
1	Woody biomass (natural gas heating)	[167]
2	Woody biomass (syngas heating)	
3	Eucalyptus waste-$ZnCl_2$	[169]
4	Eucalyptus waste-H_3PO_4	
5	Sargassum horneri	[179]
6	Exhausted olive-waste cakes	[165]
7	Sargassum horneri	[179]
8	Polyethylene terephthalate (PET) waste bottle	[163]
9	Tops + pulpwood with diesel power-remote production	[168]
10	Tops + pulpwood with power pallet-remote production	
11	Pulpwood with diesel power-remote production	
12	Pulpwood with power pallet -remote production	
13	Tops + pulpwood with grid power-in town production	
14	Tops + pulpwood with diesel power-in town production	
15	Tops + pulpwood with power pallet-in town production	
16	Pulpwood with grid power- in town production	
17	Pulpwood with diesel power- in town production	
18	Pulpwood with power pallet - in town production	
19	Pine sawdust	[171]
20	Perennial grass (Miscanthus)	[183]
21	Cattle mature	[184]

impact among the 10 impact categories selected based on normalized results, which were primarily associated with electricity consumption and the use of chemical activating agents. Homagain et al. [173] indicated that biochar application may have adverse effects on human health. Nevertheless, no definitive conclusion on the environmental impacts of PC/biochar production processes has been reached, and only a few studies have suggested that among all stages of the analyzed processes, the pyrolysis and activation stages present the most negative environmental impacts [163,169,165,179].

5.3. Novel CO_2 capture materials derived from solid waste: challenges and opportunities

Fig. 12 provides an overview of the solid waste-to-PC technology, including inputs, processing, outputs, potential applications, environmental benefits, and the necessity of LCA studies. The various FUs and system boundaries considered are the main challenges in comparing the outcomes of different LCA studies because the biomass waste-to-PC/ biochar process involves multiple product outputs and applications, including waste management, PC/biochar production, soil application, and energy generation. In particular, the inclusion of biomass growth and soil application stages may result in significant changes (i.e., GWP) in the impacts. Additionally, few studies have provided detailed contributions and hot-spot analyses, and transparent inventory data should be reported to help readers in effectively understanding the results. Furthermore, more than half of the product inventory data was generated using laboratory-scale data because the biomass waste-to-PC/ biochar process is an emerging technology. The LCA results obtained by extrapolating laboratory-scale to industrial-scale data do not accurately represent environmental impacts. In addition, most studies have considered the co-production of heat [178,170,176], bio-oil [178,173, 171] and electricity [178,176] via pyrolysis. However, the heat recovery and co-production potential have rarely been considered in studies on PC production. Finally, as stated previously, the gases released from the pyrolysis and activation processes might have significant adverse environmental impacts. However, few studies have provided detailed emission inventories for these life-cycle stages.

6. Concluding remarks and future perspectives

Carbon dioxide emissions, which are considered as the major cause of human-induced climate change [42,186], have significant impacts on the environment, including the loss of sea ice, changes in the duration and intensity of tropical storms, and an increased frequency of wildfires. Furthermore, ineffective solid waste management has led to the loss of

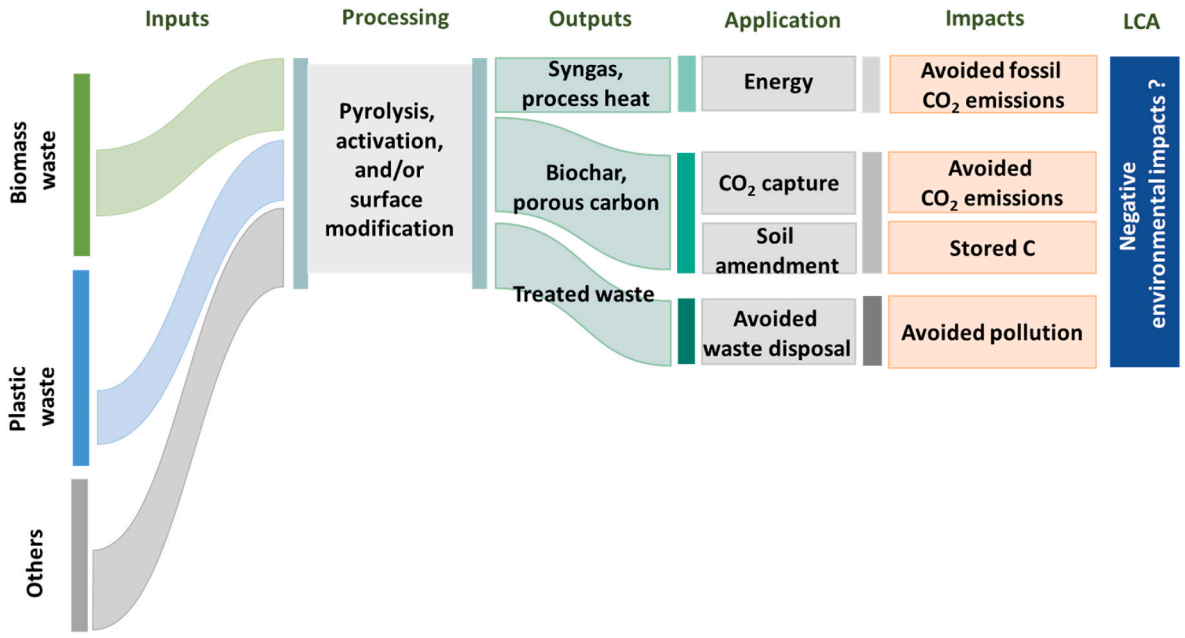

Fig. 12. Overview of the sustainable technology pathway and the necessity of LCA studies.

potentially valuable materials and caused significant environmental and health issues [23,32,187,188]. Therefore, we critically reviewed the upcycling of solid waste into PCs for CO_2 capture, which has been considered a promising and sustainable approach to simultaneously resolve these two urgent environmental issues.

First, to effectively valorize solid waste into PCs for CO_2 capture, the microporosity (particularly pore size < 0.8 nm) and surface functional groups of SWDPCs were identified as crucial factors that could be effectively enhanced by chemical activation and surface modification. The adsorption–desorption cyclic performance of CO_2 capture using SWDPCs was reviewed and evaluated through numerical simulations using several typical performance indicators, such as purity, recovery, productivity, and energy consumption-related indicators. Owing to the lack of a unified method for quantifying the energy consumption, further studies are necessary.

Second, ML-based system optimization for developing SWDPC-based CO_2 adsorption was specifically reviewed to advance CO_2 adsorption technology using solid waste as a carbon precursor. A closed-loop guideline for synthesizing PCs with excellent CO_2 capture performance was proposed, suggesting that data-driven approaches play a critical role in optimizing the synthesis of PCs for CO_2 adsorption based on the limited number of studies available thus far. When AI models were used to analyze laboratory-scale CO_2 adsorption data, it was revealed that, in addition to the adsorption conditions, textural properties were important factors for achieving high CO_2 adsorption performance, suggesting that both the intrinsic and extrinsic parameters of PCs are worth investigating with regard to SWDPC-based CO_2 adsorption. Creating a uniform database of experimental data is essential for advancing research on the application of ML to SWDPCs for CO_2 adsorption. With research progress in this direction, AI methodologies have the potential to provide an advanced and efficient platform as chemical robots for efficient, directed, and accelerated synthesis of PCs with desired properties. A closed-loop guideline, which includes smart AI techniques, facilitates the accelerated screening, design, and synthesis of SWDPCs.

Third, the environmental benefits of upcycling solid waste into PCs for CO_2 capture were comprehensively assessed via LCA. To perform an LCA on SWDPC-based CO_2 capture, different FUs and system boundaries were elaborated, and several environmental impacts, such as GWP, CED, and fossil depletion potential, were critically assessed. In addition to biomass waste, plastic waste can achieve carbon neutrality or even negative carbon emissions from a life-cycle perspective. However, the laboratory-scale CO_2 adsorption data used in many LCA studies did not provide reliable impact assessments of SWDPCs for industrial-scale applications. In addition, the LCA results were subject to changes in the system boundaries and FUs. Hence, the environmental impacts (e.g., CO_2 and toxic emissions and heavy metal pollution) of the PC synthesis processes over the entire life-cycle of the PC should be judiciously assessed when its practical applications are considered.

Comprehensive evaluations, including CO_2 adsorption, cyclic CO_2 adsorption–desorption operation, AI-based system optimization for the synthesis of CO_2 adsorbents, and LCA of the entire process, revealed that SWDPCs are promising sustainable materials for CO_2 capture that can address the issue of solid waste management. Future studies should focus on developing SWDPCs with excellent CO_2 selectivity, high CO_2 uptake at low partial pressures, stable working capacity with long cycle lifetimes, and good resistance to moisture, which can be applied for industrial-scale CO_2 adsorption. Moreover, thermochemical conversion during PC production (Fig. 2b①) and intrinsic energy consumption during CO_2 capture (Fig. 2b②) resulted in the release of CO_2. Syngas emitted from pyrolysis or gasification can be combusted to obtain thermal energy or generate electricity, whereas the CO_2 contained in it can be captured via SWDPCs. To mitigate CO_2 emissions caused by intrinsic energy consumption, viable SWDPC-based CO_2-capture approaches can be driven by hybrid renewable energy technologies (e.g., low-grade solar energy) because of their low regeneration temperatures. These approaches offer the simultaneous benefits of reduced carbon emissions and industrial-scale carbon neutrality. In addition, as real flue gases contain water and acidic gases, promising SWDPCs should exhibit high CO_2 selectivity and good resistance toward these compounds for the treatment of these gases from industrial sources.

UN SDGs are a blueprint for achieving a better and more sustainable future. To achieve these goals by 2030, urgent and effective action is required. The sustainable upcycling of solid waste into PCs for CO_2 capture has multifaceted environmental benefits, including climate change mitigation and reduction of solid waste volumes in landfills. Therefore, with a concerted effort to upcycle solid waste into CO_2 adsorbents, we are likely to meet the UN SDGs (Fig. 13), specifically *Goal 11*: Sustainable cities and communities, *Goal 12*: Responsible consumption and production, *Goal 13*: Climate action, *Goal 14*: Life below water, and *Goal 15*: Life on land.

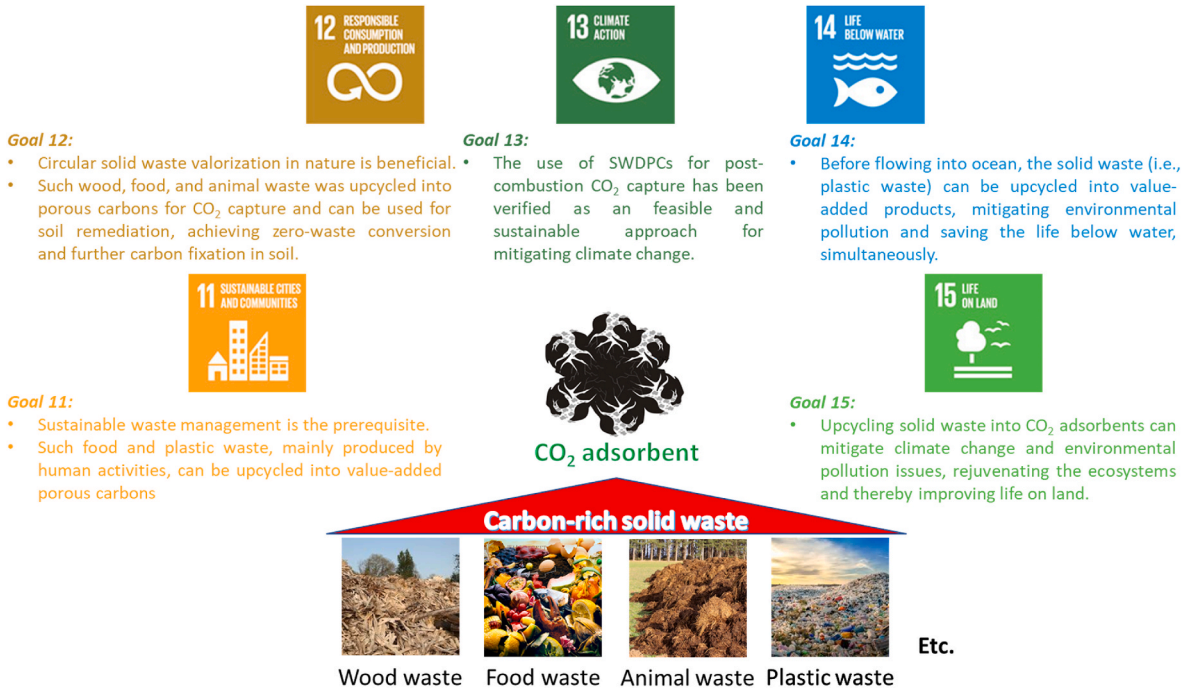

Fig. 13. Positive impacts of upcycling solid waste into CO_2 adsorbents with respect to the United Nations Sustainable Development Goals (UN SDGs).

Declaration of competing interest

The authors declare that they have no known competing financial interests or personal relationships that could have appeared to influence the work reported in this paper.

Acknowledgments

This work was supported by a National Research Foundation of Korea (NRF) grant funded by the Korean government (MSIT) (No. 2021R1A2C2011734). This research was also supported by the Basic Science Research Program through the National Research Foundation of Korea (NRF), funded by the Ministry of Education (NRF-2021R1A6A1A10045235). This research was supported by the Youth Program of the National Natural Science Foundation of China [grant number. 72104257], Natural Science and Engineering Research Council (NSERC) of Canada's Strategic Partnership Program, U.S. National Science Foundation AccelNet Program [grant number 1927336], and Saudi Aramco. The authors are grateful to all the funding agencies and sponsors for their support.

References

[1] Gloabl Monitoring Laboratory. National Oceanic and Atmospheric Administration. Trends in atmospheric carbon dioxide. 2020.
[2] Olivares-Marín M, Maroto-Valer MM. Development of adsorbents for CO_2 capture from waste materials: a review. Greenh Gases: Sci Technol 2012;2:20–35.
[3] Wang J, Huang L, Yang R, Zhang Z, Wu J, Gao Y, et al. Recent advances in solid sorbents for CO_2 capture and new development trends. Energy Environ Sci 2014;7:3478–518.
[4] Oschatz M, Antonietti M. A search for selectivity to enable CO_2 capture with porous adsorbents. Energy Environ Sci 2018;11:57–70.
[5] Wang Q, Luo J, Zhong Z, Borgna A. CO_2 capture by solid adsorbents and their applications: current status and new trends. Energy Environ Sci 2011;4:42–55.
[6] WMO. World Meteorological Organization (WMO). Statement on the state of the global climate in 2018. World Meteorological Organization; 2019.
[7] Masson-Delmotte V, Zhai P, Pörtner H-O, Roberts D, Skea J, et al. Global Warming of 1.5 °C. Intergovernmental Panel on Climate Change; 2018.
[8] Coll Carolina, Gibbins Jon, Heiberg Sigurd, Heidug Wolfgang, Hicks Denis, Alexander Krowka, et al. Carbon carpture, use and storage (CCUS). United Nations Economic Commission for Europe (UNECE); 2021.
[9] Le Quéré C, Jackson RB, Jones MW, Smith AJP, Abernethy S, Andrew RM, et al. Temporary reduction in daily global CO_2 emissions during the COVID-19 forced confinement. Nat Clim Change 2020;10:647–53.
[10] Igalavithana AD, Choi SW, Shang J, Hanif A, Dissanayake PD, Tsang DCW, et al. Carbon dioxide capture in biochar produced from pine sawdust and paper mill sludge: effect of porous structure and surface chemistry. Sci Total Environ 2020;739:139845.
[11] MacDowell N, Florin N, Buchard A, Hallett J, Galindo A, Jackson G, et al. An overview of CO_2 capture technologies. Energy Environ Sci 2010;3:1645–69.
[12] Markewitz P, Kuckshinrichs W, Leitner W, Linssen J, Zapp P, Bongartz R, et al. Worldwide innovations in the development of carbon capture technologies and the utilization of CO_2. Energy Environ Sci 2012;5:7281–305.
[13] Overa S, Feric TG, Park A-HA, Jiao F. Tandem and hybrid processes for carbon dioxide utilization. Joule 2021;5:8–13.
[14] Rim G, Feric TG, Moore T, Park AHA. Solvent impregnated polymers loaded with liquid-like nanoparticle organic hybrid materials for enhanced kinetics of direct air capture and point source CO_2 capture. Adv Funct Mater 2021;31:2010047.
[15] Wang J, Petit C, Zhang X, Park A-HA. Simultaneous measurement of CO_2 sorption and swelling of phosphate-based ionic liquid. Green Energy Environ 2016;1:258–65.
[16] Petit C, Lin KY, Park AH. Design and characterization of liquidlike POSS-based hybrid nanomaterials synthesized via ionic bonding and their interactions with CO_2. Langmuir 2013;29:12234–42.
[17] Ochedi FO, Liu Y, Adewuyi YG. State-of-the-art review on capture of CO_2 using adsorbents prepared from waste materials. Process Saf Environ Protect 2020;139:1–25.
[18] Wang J, Yang Y, Jia Q, Shi Y, Guan Q, Yang N, et al. Solid-waste-derived carbon dioxide-capturing materials. ChemSusChem 2019;12:2055–82.
[19] Creamer AE, Gao B. Carbon-based adsorbents for postcombustion CO_2 capture: a critical review. Environ Sci Technol 2016;50:7276–89.
[20] Igalavithana AD, Choi SW, Dissanayake PD, Shang J, Wang CH, Yang X, et al. Gasification biochar from biowaste (food waste and wood waste) for effective CO_2 adsorption. J Hazard Mater 2020;391:121147.
[21] Krza Sy L, Bhada-Tata P, Van Woerden F. What a waste 2.0-A global snapshot of solid waste management to 2050. World Bank Group; 2018.
[22] Wilson DC, Rodic L, Modak P, et al. Global Waste Management Outlook. United Nations Environment Programme; 2015.
[23] You S, Sonne C, Ok YS. COVID-19's unsustainable waste management. Science 2020;368:1438.
[24] Janice Brahney MH, Heim Eric, Hahnenberger Maura, Sukumaran Suja. Plastic rain in protected areas of the United States. Science 2020;368:1257–60.
[25] Bank MS, Hansson SV. The plastic cycle: a novel and holistic paradigm for the anthropocene. Environ Sci Technol 2019;53:7177–9.
[26] Joleah B, Lamb BLW, Fiorenza Evan A, Couch Courtney S, Howard Robert, Rader Douglas N, True James D, Kelly Lisa A, Ahmad Awaludinnoer, Jompa Jamaluddin, Drew Harvell C. Plastic waste associated with disease on coral reefs. Science 2018;359:460–2.
[27] MacArthur E. Beyond plastic waste. Science 2017;358:843.

[28] Allen S, Allen D, Phoenix VR, Le Roux G, Durántez Jiménez P, Simonneau A, et al. Atmospheric transport and deposition of microplastics in a remote mountain catchment. Nat Geosci 2019;12:339–44.

[29] Cox KD, Covernton GA, Davies HL, Dower JF, Juanes F, Dudas SE. Human consumption of microplastics. Environ Sci Technol 2019;53:7068–74.

[30] You S, Sonne C, Ok YS, Alessi D. COVID-19: resource recovery from plastic waste against plastic pollution. Cogent Environmental Science 2020;6:1801220.

[31] Li C, Yuan X, Sun Z, Suvarna M, Hu X, Wang X, et al. Pyrolysis of waste surgical masks into liquid fuel and its life-cycle assessment. Bioresour Technol 2022;346:126582. https://doi.org/10.1016/j.biortech.2021.126582.

[32] Yuan X, Wang X, Sarkar B, Ok YS. The COVID-19 pandemic necessitates a shift to a plastic circular economy. Nat Rev Earth Environ 2021;2:659–60. https://doi.org/10.1038/s43017-021-00223-2.

[33] Nolan Nanthi S, Kirkham MB, Halsband Claudia, Nygegoda Dayanthi, Ok YS. Particulate Plastics in Terrestrial and Aquatic Environments. first ed. Boca Raton: Taylor & Francis Group; 2020.

[34] Dissanayake PD, You S, Igalavithana AD, et al. Biochar-based adsorbents for carbon dioxide capture: A critical review. Renew Sustain Energy Rev 2020;119:109582.

[35] Kaithwas A, Prasad M, Kulshreshtha A, Verma S. Industrial wastes derived solid adsorbents for CO_2 capture: a mini review. Chem Eng Res Des 2012;90:1632–41.

[36] Lee S-Y, Park S-J. A review on solid adsorbents for carbon dioxide capture. J Ind Eng Chem 2015;23:1–11.

[37] Rashidi NA, Yusup S. An overview of activated carbons utilization for the post-combustion carbon dioxide capture. J CO2 Util 2016;13:1–16.

[38] Zhao H, Luo X, Zhang H, Sun N, Wei W, Sun Y. Carbon-based adsorbents for post-combustion capture: a review. Greenh Gases: Sci Technol 2018;8:11–36.

[39] Singh G, Lakhi KS, Sil S, Bhosale SV, Kim I, Albahily K, et al. Biomass derived porous carbon for CO_2 capture. Carbon 2019;148:164–86.

[40] Zhou X-L, Zhang H, Shao L-M, Lü F, He P-J. Preparation and application of hierarchical porous carbon materials from waste and biomass: a review. Waste Biomass Valorization 2020;12:1699–724.

[41] Li S, Yuan X, Deng S, Zhao L, Lee KB. A review on biomass-derived CO_2 adsorption capture: Adsorbent, adsorber, adsorption, and advice. Renew Sustain Energy Rev 2021;152:111708. https://doi.org/10.1016/j.rser.2021.111708.

[42] Yuan X, Suvarna M, Low S, Dissanayake PD, Lee KB, Li J, et al. Applied machine learning for prediction of CO_2 adsorption on biomass waste-derived porous carbons. Environ Sci Technol 2021;55(17):11925–36.

[43] Liu WJ, Jiang H, Yu HQ. Development of biochar-based functional materials: toward a sustainable platform carbon material. Chem Rev 2015;115:12251–85.

[44] Panwar NL, Kothari R, Tyagi VV. Thermo chemical conversion of biomass – eco friendly energy routes. Renew Sustain Energy Rev 2012;16:1801–16.

[45] Yuan X, Dissanayake PD, Gao B, Liu WJ, Lee KB, Ok YS. Review on upgrading organic waste to value-added carbon materials for energy and environmental applications. J Environ Manag 2021;296:113128.

[46] Li J, Zhu X, Li Y, Tong YW, Ok YS, Wang X. Multi-task prediction and optimization of hydrochar properties from high-moisture municipal solid waste: application of machine learning on waste-to-resource. J Clean Prod 2021;278:123928.

[47] Li Q, Zhang S, Gholizadeh M, Hu X, Yuan X, et al. Co-hydrothermal carbonization of swine and chicken manure: Influence of cross-interaction on hydrochar and liquid characteristics. Sci Total Environ 2021;786:147381.

[48] Tripathi M, Sahu JN, Ganesan P. Effect of process parameters on production of biochar from biomass waste through pyrolysis: a review. Renew Sustain Energy Rev 2016;55:467–81.

[49] Yang X, Ng W, Wong BSE, Baeg GH, Wang CH, Ok YS. Characterization and ecotoxicological investigation of biochar produced via slow pyrolysis: effect of feedstock composition and pyrolysis conditions. J Hazard Mater 2019;365:178–85.

[50] Lam SS, Liew RK, Wong YM, Yek PNY, Ma NL, Lee CL, et al. Microwave-assisted pyrolysis with chemical activation, an innovative method to convert orange peel into activated carbon with improved properties as dye adsorbent. J Clean Prod 2017;162:1376–87.

[51] Ao W, Fu J, Mao X, Kang Q, Ran C, Liu Y, et al. Microwave assisted preparation of activated carbon from biomass: a review. Renew Sustain Energy Rev 2018;92:958–79.

[52] Lam SS, Yek PNY, Ok YS, Chong CC, Liew RK, Tsang DCW, et al. Engineering pyrolysis biochar via single-step microwave steam activation for hazardous landfill leachate treatment. J Hazard Mater 2020;390:121649.

[53] Wei L, Sevilla M, Fuertes AB, Mokaya R, Yushin G. Hydrothermal carbonization of abundant renewable natural organic chemicals for high-performance supercapacitor electrodes. Adv Energy Mater 2011;1:356–61.

[54] Sun Y, Gao B, Yao Y, Fang J, Zhang M, Zhou Y, et al. Effects of feedstock type, production method, and pyrolysis temperature on biochar and hydrochar properties. Chem Eng J 2014;240:574–8.

[55] Kambo HS, Dutta A. A comparative review of biochar and hydrochar in terms of production, physico-chemical properties and applications. Renew Sustain Energy Rev 2015;45:359–78.

[56] Liu W-J, Jiang H, Yu H-Q. Emerging applications of biochar-based materials for energy storage and conversion. Energy Environ Sci 2019;12:1751–79.

[57] Danish M, Ahmad T. A review on utilization of wood biomass as a sustainable precursor for activated carbon production and application. Renew Sustain Energy Rev 2018;87:1–21.

[58] Tan XF, Liu SB, Liu YG, Gu YL, Zeng GM, Hu XJ, et al. Biochar as potential sustainable precursors for activated carbon production: multiple applications in environmental protection and energy storage. Bioresour Technol 2017;227:359–72.

[59] Premarathna KSD, Rajapaksha AU, Sarkar B, Kwon EE, Bhatnagar A, Ok YS, et al. Biochar-based engineered composites for sorptive decontamination of water: a review. Chem Eng J 2019;372:536–50.

[60] Liu SF, Ma R, Hu X, Wang LL, Wang XY, Radosz M, et al. CO_2 adsorption on hazelnut-shell-derived nitrogen-doped porous carbons synthesized by single-step sodium amide activation. Ind Eng Chem Res 2020;59:7046–53.

[61] Chen C, Kim J, Ahn W-S. CO_2 capture by amine-functionalized nanoporous materials: a review. Kor J Chem Eng 2014;31:1919–34.

[62] González-García P. Activated carbon from lignocellulosics precursors: a review of the synthesis methods, characterization techniques and applications. Renew Sustain Energy Rev 2018;82:1393–414.

[63] Fang J, Gao B, Zimmerman AR, Ro KS, Chen J. Physically (CO_2) activated hydrochars from hickory and peanut hull: preparation, characterization, and sorption of methylene blue, lead, copper, and cadmium. RSC Adv 2016;6:24906–11.

[64] Yuan X, Choi SW, Jang E, Lee KB. Chemically activated microporous carbons derived from petroleum coke: performance evaluation for CF_4 adsorption. Chem Eng J 2018;336:297–305.

[65] Thines KR, Abdullah EC, Mubarak NM, Ruthiraan M. Synthesis of magnetic biochar from agricultural waste biomass to enhancing route for waste water and polymer application: a review. Renew Sustain Energy Rev 2017;67:257–76.

[66] Yuan X, Li S, Jeon S, Deng S, Zhao L, Lee KB. Valorization of waste polyethylene terephthalate plastic into N-doped microporous carbon for CO_2 capture through a one-pot synthesis. J Hazard Mater 2020;399:123010.

[67] Yuan X, Lee JG, Yun H, Deng S, Kim YJ, Lee JE, et al. Solving two environmental issues simultaneously: waste polyethylene terephthalate plastic bottle-derived microporous carbons for capturing CO_2. Chem Eng J 2020;397:125350. https://doi.org/10.1016/j.cej.2020.125350.

[68] Sun H, Yang B, Li A. Biomass derived porous carbon for efficient capture of carbon dioxide, organic contaminants and volatile iodine with exceptionally high uptake. Chem Eng J 2019;372:65–73.

[69] Wei H, Chen J, Fu N, Chen H, Lin H, Han S. Biomass-derived nitrogen-doped porous carbon with superior capacitive performance and high CO_2 capture capacity. Electrochim Acta 2018;266:161–9.

[70] Wu D, Liu J, Yang Y, Zheng Y. Nitrogen/oxygen Co-doped porous carbon derived from biomass for low-pressure CO_2 capture. Ind Eng Chem Res 2020;59:14055–63.

[71] Guo L, Yang J, Hu G, Hu X, Wang L, Dong Y, et al. Role of hydrogen peroxide preoxidizing on CO_2 adsorption of nitrogen-doped carbons produced from coconut shell. ACS Sustainable Chem Eng 2016;4:2806–13.

[72] Geng Z, Xiao Q, Lv H, Li B, Wu H, Lu Y, et al. One-step synthesis of microporous carbon monoliths derived from biomass with high nitrogen doping content for highly selective CO_2 capture. Sci Rep 2016;6:30049.

[73] Serafin J, Narkiewicz U, Morawski AW, Wróbel RJ, Michalkiewicz B. Highly microporous activated carbons from biomass for CO_2 capture and effective micropores at different conditions. J CO2 Util 2017;18:73–9.

[74] Pevida C, Plaza MG, Arias B, Fermoso J, Rubiera F, Pis JJ. Surface modification of activated carbons for CO_2 capture. Appl Surf Sci 2008;254:7165–72.

[75] Shafeeyan MS, Daud WMAW, Houshmand A, Shamiri A. A review on surface modification of activated carbon for carbon dioxide adsorption. J Anal Appl Pyrol 2010;89:143–51.

[76] Nazir G, Rehman A, Park S-J. Role of heteroatoms (nitrogen and sulfur)-dual doped corn-starch based porous carbons for selective CO_2 adsorption and separation. J CO2 Util 2021;51:101641.

[77] Ma X, Li L, Zeng Z, Chen R, Wang C, Zhou K, et al. Experimental and theoretical demonstration of the relative effects of O-doping and N-doping in porous carbons for CO_2 capture. Appl Surf Sci 2019;481:1139–47.

[78] Mondal AK, Kretschmer K, Zhao Y, Liu H, Fan H, Wang G. Naturally nitrogen doped porous carbon derived from waste shrimp shells for high-performance lithium ion batteries and supercapacitors. Microporous Mesoporous Mater 2017;246:72–80.

[79] Han X, Jiang H, Zhou Y, Hong W, Zhou Y, Gao P, et al. A high performance nitrogen-doped porous activated carbon for supercapacitor derived from pueraria. J Alloys Compd 2018;744:544–51.

[80] Du W, Wang X, Sun X, Zhan J, Zhang H, Zhao X. Nitrogen-doped hierarchical porous carbon using biomass-derived activated carbon/carbonized polyaniline composites for supercapacitor electrodes. J Electroanal Chem 2018;827:213–20.

[81] Li Y, Wang G, Wei T, Fan Z, Yan P. Nitrogen and sulfur co-doped porous carbon nanosheets derived from willow catkin for supercapacitors. Nano Energy 2016;19:165–75.

[82] Zhao Z-Q, Xiao P-W, Zhao L, Liu Y, Han B-H. Human hair-derived nitrogen and sulfur co-doped porous carbon materials for gas adsorption. RSC Adv 2015;5:73980–8.

[83] Li G, Li Y, Chen X, Hou X, Lin H, Jia L. One step synthesis of N, P co-doped hierarchical porous carbon nanosheets derived from pomelo peel for high performance supercapacitors. J Colloid Interface Sci 2021;605:71–81.

[84] Liu WJ, Jiang H, Tian K, Ding YW, Yu HQ. Mesoporous carbon stabilized MgO nanoparticles synthesized by pyrolysis of $MgCl_2$ preloaded waste biomass for highly efficient CO_2 capture. Environ Sci Technol 2013;47:9397–403.

[85] Lahijani P, Mohammadi M, Mohamed AR. Metal incorporated biochar as a potential adsorbent for high capacity CO_2 capture at ambient condition. J CO2 Util 2018;26:281–93.

[86] Shahkarami S, Dalai AK, Soltan J. Enhanced CO_2 adsorption using MgO-impregnated activated carbon: impact of preparation techniques. Ind Eng Chem Res 2016;55:5955–64.
[87] Singh G, Lee J, Karakoti A, Bahadur R, Yi J, Zhao D, et al. Emerging trends in porous materials for CO_2 capture and conversion. Chem Soc Rev 2020;49:4360–404.
[88] Patel HA, Je SH, Park J, Chen DP, Jung Y, Yavuz CT, et al. Unprecedented high-temperature CO_2 selectivity in N_2-phobic nanoporous covalent organic polymers. Nat Commun 2013;4:1357.
[89] Choi SW, Tang J, Pol VG, Lee KB. Pollen-derived porous carbon by KOH activation: effect of physicochemical structure on CO_2 adsorption. J CO2 Util 2019;29:146–55.
[90] Babu DJ, Bruns M, Schneider R, Gerthsen D, Schneider JJ. Understanding the influence of N-doping on the CO_2 adsorption characteristics in carbon nanomaterials. J Phys Chem C 2017;121:616–26.
[91] Seema H, Kemp KC, Le NH, Park S-W, Chandra V, Lee JW, et al. Highly selective CO_2 capture by S-doped microporous carbon materials. Carbon 2014;66:320–6.
[92] Kaur B, Singh J, Gupta RK, Bhunia H. Porous carbons derived from polyethylene terephthalate (PET) waste for CO_2 capture studies. J Environ Manag 2019;242:68–80.
[93] Yuan X, Kumar NM, Brigljević B, Li S, Deng S, Byun M, et al. Sustainability-inspired upcycling of waste polyethylene terephthalate plastic into porous carbon for CO_2 capture. Green Chem 2022;24:1494–504.
[94] Hong S-M, Yoon HJ, Choi Y, Cho Y-Z, Mun S, Pol VG, et al. Solving two environmental problems simultaneously: scalable production of carbon microsheets from structured packing peanuts with tailored microporosity for efficient CO_2 capture. Chem Eng J 2020;379:122219.
[95] Idrees M, Rangari V, Jeelani S. Sustainable packaging waste- derived activated carbon for carbon dioxide capture. J CO2 Util 2018;26:380–7.
[96] Kim M-J, Choi SW, Kim H, Mun S, Lee KB. Simple synthesis of spent coffee ground-based microporous carbons using K_2CO_3 as an activation agent and their application to CO_2 capture. Chem Eng J 2020:397.
[97] Liu SH, Huang YY. Valorization of coffee grounds to biochar-derived adsorbents for CO_2 adsorption. J Clean Prod 2018;175:354–60.
[98] Boyjoo Y, Cheng Y, Zhong H, Tian H, Pan J, Pareek VK, et al. From waste Coca Cola® to activated carbons with impressive capabilities for CO_2 adsorption and supercapacitors. Carbon 2017;116:490–9.
[99] Choma J, Marszewski M, Osuchowski L, Jagiello J, Dziura A, Jaroniec M. Adsorption properties of activated carbons prepared from waste CDs and DVDs. ACS Sustainable Chem Eng 2015;3:733–42.
[100] Jang E, Choi SW, Hong S-M, Shin S, Lee KB. Development of a cost-effective CO_2 adsorbent from petroleum coke via KOH activation. Appl Surf Sci 2018;429:62–71.
[101] Jang E, Choi SW, Lee KB. Effect of carbonization temperature on the physical properties and CO_2 adsorption behavior of petroleum coke-derived porous carbon. Fuel 2019;248:85–92.
[102] Dissanayake PD, Choi SW, Igalavithana AD, Yang X, Tsang DCW, Wang C-H, et al. Sustainable gasification biochar as a high efficiency adsorbent for CO_2 capture: a facile method to designer biochar fabrication. Renew Sustain Energy Rev 2020;124:109785.
[103] Nowrouzi M, Younesi H, Bahramifar N. Superior CO_2 capture performance on biomass-derived carbon/metal oxides nanocomposites from Persian ironwood by H_3PO_4 activation. Fuel 2018;223:99–114.
[104] Sivadas DL, Damodaran A, Raghavan R. Microporous carbon monolith and fiber from freeze-dried banana stems for high efficiency carbon dioxide adsorption. ACS Sustainable Chem Eng 2019;7:12807–16.
[105] Hirst EA, Taylor A, Mokaya R. A simple flash carbonization route for conversion of biomass to porous carbons with high CO_2 storage capacity. J Mater Chem 2018;6:12393–403.
[106] Balahmar N, Mitchell AC, Mokaya R. Generalized mechanochemical synthesis of biomass-derived sustainable carbons for high performance CO_2 Storage. Adv Energy Mater 2015;5(22):1500867.
[107] Yang J, Yue L, Hu X, Wang L, Zhao Y, Lin Y, et al. Efficient CO_2 capture by porous carbons derived from coconut shell. Energy Fuel 2017;31:4287–93.
[108] Ello AS, de Souza LKC, Trokourey A, Jaroniec M. Coconut shell-based microporous carbons for CO_2 capture. Microporous Mesoporous Mater 2013;180:280–3.
[109] Yue L, Xia Q, Wang L, Wang L, DaCosta H, Yang J, et al. CO_2 adsorption at nitrogen-doped carbons prepared by K_2CO_3 activation of urea-modified coconut shell. J Colloid Interface Sci 2018;511:259–67.
[110] Chen J, Yang J, Hu GS, Hu X, Li ZM, Shen SW, et al. Enhanced CO_2 capture capacity of nitrogen-doped biomass-derived porous carbons. ACS Sustainable Chem Eng 2016;4:1439–45.
[111] Yang M, Guo L, Hu G, Hu X, Xu L, Chen J, et al. Highly cost-effective nitrogen-doped porous coconut shell-based CO_2 sorbent synthesized by combining ammoxidation with KOH activation. Environ Sci Technol 2015;49:7063–70.
[112] Boujibar O, Souikny A, Ghamouss F, Achak O, Dahbi M, Chafik T. CO_2 capture using N-containing nanoporous activated carbon obtained from argan fruit shells. J Environ Chem Eng 2018;6:1995–2002.
[113] Xu Y, Yang Z, Zhang G, Zhao P. Excellent CO_2 adsorption performance of nitrogen-doped waste biocarbon prepared with different activators. J Clean Prod 2020;264:121645.
[114] Yang Z, Zhang G, Xu Y, Zhao P. One step N-doping and activation of biomass carbon at low temperature through $NaNH_2$: an effective approach to CO_2 adsorbents. J CO2 Util 2019;33:320–9.
[115] Rouzitalab Z, Mohammady Maklavany D, Rashidi A, Jafarinejad S. Synthesis of N-doped nanoporous carbon from walnut shell for enhancing CO_2 adsorption capacity and separation. J Environ Chem Eng 2018;6:6653–63.
[116] Yang F, Wang J, Liu L, Zhang P, Yu W, Deng Q, et al. Synthesis of porous carbons with high N-content from shrimp shells for efficient CO_2-capture and gas separation. ACS Sustainable Chem Eng 2018;6:15550–9.
[117] Rao L, Liu S, Wang L, Ma C, Wu J, An L, et al. N-doped porous carbons from low-temperature and single-step sodium amide activation of carbonized water chestnut shell with excellent CO_2 capture performance. Chem Eng J 2019;359:428–35.
[118] Gao A, Guo N, Yan M, Li M, Wang F, Yang R. Hierarchical porous carbon activated by $CaCO_3$ from pigskin collagen for CO_2 and H_2 adsorption. Microporous Mesoporous Mater 2018;260:172–9.
[119] Chang B, Shi W, Yin H, Zhang S, Yang B. Poplar catkin-derived self-templated synthesis of N-doped hierarchical porous carbon microtubes for effective CO_2 capture. Chem Eng J 2019;358:1507–18.
[120] Zhu MY, Cai WQ, Verpoort F, Zhou JB. Preparation of pineapple waste-derived porous carbons with enhanced CO_2 capture performance by hydrothermal carbonation-alkali metal oxalates assisted thermal activation process. Chem Eng Res Des 2019;146:130–40.
[121] Huang G-G, Liu Y-F, Wu X-X, Cai J-J. Activated carbons prepared by the KOH activation of a hydrochar from garlic peel and their CO_2 adsorption performance. N Carbon Mater 2019;34:247–57.
[122] Zhu B, Qiu K, Shang C, Guo Z. Naturally derived porous carbon with selective metal- and/or nitrogen-doping for efficient CO_2 capture and oxygen reduction. J Mater Chem 2015;3:5212–22.
[123] Han J, Zhang L, Zhao B, Qin L, Wang Y, Xing F. The N-doped activated carbon derived from sugarcane bagasse for CO_2 adsorption. Ind Crop Prod 2019;128:290–7.
[124] Yue L, Rao L, Wang L, Wang L, Wu J, Hu X, et al. Efficient CO_2 capture by nitrogen-doped biocarbons derived from rotten strawberries. Ind Eng Chem Res 2017;56:14115–22.
[125] Coromina HM, Walsh DA, Mokaya R. Biomass-derived activated carbon with simultaneously enhanced CO_2 uptake for both pre and post combustion capture applications. J Mater Chem 2016;4:280–9.
[126] Alabadi A, Razzaque S, Yang Y, Chen S, Tan B. Highly porous activated carbon materials from carbonized biomass with high CO_2 capturing capacity. Chem Eng J 2015;281:606–12.
[127] Li D, Ma T, Zhang R, Tian Y, Qiao Y. Preparation of porous carbons with high low-pressure CO_2 uptake by KOH activation of rice husk char. Fuel 2015;139:68–70.
[128] Liu X, Sun C, Liu H, Tan WH, Wang W, Snape C. Developing hierarchically ultra-micro/mesoporous biocarbons for highly selective carbon dioxide adsorption. Chem Eng J 2019;361:199–208.
[129] Zhu B, Shang C, Guo Z. Naturally nitrogen and calcium-doped nanoporous carbon from pine cone with superior CO_2 capture capacities. ACS Sustainable Chem Eng 2016;4:1050–7.
[130] Xu X, Xu Z, Gao B, Zhao L, Zheng Y, Huang J, et al. New insights into CO_2 sorption on biochar/Fe oxyhydroxide composites: kinetics, mechanisms, and in situ characterization. Chem Eng J 2020:384.
[131] Pennline HW. Sorbent research for the Capture of Carbon Dioxide. NETL Technical Report Series. U.S. Department of Energy, National Energy Technology Laboratory; 2016.
[132] Raganati F, Chirone R, Ammendola P. CO_2 capture by temperature swing adsorption: working capacity as affected by temperature and CO_2 partial pressure. Ind Eng Chem Res 2020;59:3593–605.
[133] Zhang Z, Xiao Y, Wang B, Sun Q, Liu H. Waste is a misplayed resource: synthesis of zeolites from fly ash for CO_2 capture. Energy Proc 2017;114:2537–44.
[134] Mallesh D, Anbarasan J, Mahesh Kumar P, Upendar K, Chandrashekar P, Rao BVSK, et al. Synthesis, characterization of carbon adsorbents derived from waste biomass and its application to CO_2 capture. Appl Surf Sci 2020:530.
[135] Plaza MG, González AS, Pevida C, Pis JJ, Rubiera F. Valorisation of spent coffee grounds as CO_2 adsorbents for postcombustion capture applications. Appl Energy 2012;99:272–9.
[136] Tiwari D, Goel C, Bhunia H, Bajpai PK. Melamine-formaldehyde derived porous carbons for adsorption of CO_2 capture. J Environ Manag 2017;197:415–27.
[137] Kaur B, Gupta RK, Bhunia H. Chemically activated nanoporous carbon adsorbents from waste plastic for CO_2 capture: breakthrough adsorption study. Microporous Mesoporous Mater 2019;282:146–58.
[138] Olajire AA. CO_2 capture and separation technologies for end-of-pipe applications – a review. Energy 2010;35:2610–28.
[139] Rouzitalab Z, Maklavany DM, Jafarinejad S, Rashidi A. Lignocellulose-based adsorbents: a spotlight review of the effective parameters on carbon dioxide capture process. Chemosphere 2020;246:125756.
[140] Karimi M, Zafanelli LFAS, Almeida JPP, Ströher GR, Rodrigues AE, Silva JAC. Novel insights into activated carbon derived from municipal solid waste for CO_2 uptake: synthesis, adsorption isotherms and scale-up. J Environ Chem Eng 2020;8(5):104069.
[141] Horstmeier JF, Gomez Lopez A, Agar DW. Performance improvement of vacuum swing adsorption processes for CO_2 removal with integrated phase change material. Int J Greenh Gas Control 2016;47:364–75.
[142] Bahamon D, Ogungbenro AE, Khaleel M, Abu-Zahra MRM, Vega LF. Performance of activated carbons derived from date seeds in CO_2 swing adsorption determined by combining experimental and molecular simulation data. Ind Eng Chem Res 2020;59:7161–73.

[143] Plaza MG, Rubiera F. Development of carbon-based vacuum, temperature and concentration swing adsorption post-combustion CO_2 capture processes. Chem Eng J 2019;375:122002.
[144] Zhao J, Deng S, Zhao L, Yuan X, Du Z, Li S, et al. Understanding the effect of H_2O on CO_2 adsorption capture: mechanism explanation, quantitative approach and application. Sustain Energy Fuels 2020;4:5970–86.
[145] Zhao J, Deng S, Zhao L, Yuan X, Wang B, Chen L, et al. Synergistic and competitive effect of H_2O on CO_2 adsorption capture: mechanism explanations based on molecular dynamic simulation. J CO2 Util 2021:52.
[146] Li J, Lim K, Yang H, Ren Z, Raghavan S, Chen P-Y, et al. AI applications through the whole life cycle of material discovery. Matter 2020;3:393–432.
[147] Fanourgakis GS, Gkagkas K, Tylianakis E, Froudakis GE. A universal machine learning algorithm for large-scale screening of materials. J Am Chem Soc 2020; 142:3814–22.
[148] Medford AJ, Kunz MR, Ewing SM, Borders T, Fushimi R. Extracting knowledge from data through catalysis informatics. ACS Catal 2018;8:7403–29.
[149] Lookman T, Balachandran PV, Xue D, Yuan R. Active learning in materials science with emphasis on adaptive sampling using uncertainties for targeted design. npj Comput Mater 2019;5:21.
[150] Fernandez M, Boyd PG, Daff TD, Aghaji MZ, Woo TK. Rapid and accurate machine learning recognition of high performing metal organic frameworks for CO_2 capture. J Phys Chem Lett 2014;5:3056–60.
[151] Li J, Suvarna M, Tong YW, Wang X. Fuel properties of hydrochar and pyrochar: Prediction and exploration with machine learning. Appl Energy 2020;269: 115166.
[152] Zhu X, Tsang DCW, Wang L, Su Z, Hou D, Li L, et al. Machine learning exploration of the critical factors for CO_2 adsorption capacity on porous carbon materials at different pressures. J Clean Prod 2020;273:122915.
[153] Wang S, Zhang Z, Dai S, Jiang D-e. Insights into CO_2/N_2 selectivity in porous carbons from deep learning. ACS Mater Lett 2019;1:558–63.
[154] Wang S, Li Y, Dai S, Jiang DE. Prediction by convolutional neural networks of CO_2/N_2 selectivity in porous carbons from N_2 adsorption isotherm at 77 K. Angew Chem Int Ed 2020;59:19645–8.
[155] Borboudakis G, Stergiannakos T, Frysali M, Klontzas E, Tsamardinos I, Froudakis GE. Chemically intuited, large-scale screening of MOFs by machine learning techniques. npj Comput Mater 2017;3:40.
[156] Tsamardinos I, Fanourgakis GS, Greasidou E, Klontzas E, Gkagkas K, Froudakis GE. An Automated Machine Learning architecture for the accelerated prediction of Metal-Organic Frameworks performance in energy and environmental applications. Microporous Mesoporous Mater 2020;300:110160.
[157] Gaillac R, Chibani S, Coudert F-X. Speeding up discovery of auxetic zeolite frameworks by machine learning. Chem Mater 2020;32:2653–63.
[158] Evans JD, Coudert F-X. Predicting the mechanical properties of zeolite frameworks by machine learning. Chem Mater 2017;29:7833–9.
[159] Jensen Z, Kim E, Kwon S, Gani TZH, Roman-Leshkov Y, Moliner M, et al. A machine learning approach to zeolite synthesis enabled by automatic literature data extraction. ACS Cent Sci 2019;5:892–9.
[160] Jain A, Persson KA, Ceder G. Research Update: the materials genome initiative: data sharing and the impact of collaborative *ab initio* databases. Apl Mater 2016; 4:053102.
[161] Coley CW, Thomas 3rd DA, Lummiss JAM, Jaworski JN, Breen CP, Schultz V, et al. A robotic platform for flow synthesis of organic compounds informed by AI planning. Science 2019;365:557.
[162] Granda JM, Donina L, Dragone V, Long DL, Cronin L. Controlling an organic synthesis robot with machine learning to search for new reactivity. Nature 2018; 559:377–81.
[163] Wang J, Yuan X, Deng S, Zeng X, Yu Z, Li S, et al. Waste polyethylene terephthalate (PET) plastics-derived activated carbon for CO_2 capture: a route to a closed carbon loop. Green Chem 2020;22:6836–45. https://doi.org/10.1039/D0GC01613F.
[164] Arena N, Lee J, Clift R. Life Cycle Assessment of activated carbon production from coconut shells. J Clean Prod 2016;125:68–77.
[165] Hjaila K, Baccar R, Sarra M, Gasol CM, Blanquez P. Environmental impact associated with activated carbon preparation from olive-waste cake via life cycle assessment. J Environ Manag 2013;130:242–7.
[166] Loya-Gonzalez D, Loredo-Cancino M, Soto-Regalado E, Rivas-Garcia P, de Jesus Cerino-Cordova F, Bernardo Garcia-Reyes R, et al. Optimal activated carbon production from corn pericarp: a life cycle assessment approach. J Clean Prod 2019;219:316–25.
[167] Bergman R, Gu H, Alanya-Rosenbaum S, Liang S. Comparative life-cycle assessment of biochar activated carbon and synthesis gas electricity with commercially available alternatives. United States Department of Agriculture; 2019. p. 32.
[168] Puettmann ME, Sahoo K, Wilson K, Oneil E. Life cycle assessment of biochar produced from forest residues using portable systems. J Clean Prod 2020;250: 119564.
[169] Heidari A, Khaki E, Younesi H, Lu HR. Evaluation of fast and slow pyrolysis methods for bio-oil and activated carbon production from eucalyptus wastes using a life cycle assessment approach. J Clean Prod 2019;241:118394.
[170] Roberts KG, Gloy BA, Joseph S, Scott NR, Lehmann J. Life cycle assessment of biochar systems: estimating the energetic, economic, and climate change potential. Environ Sci Technol 2010;44:827–33.
[171] Hersh B, Mirkouei A. Life cycle assessment OF pyrolysis-derived biochar from organic wastes and advanced feedstocks. In: Proceedings of the ASME; 2019.
[172] Pierobon F, Eastin IL, Ganguly I. Life cycle assessment of residual lignocellulosic biomass-based jet fuel with activated carbon and lignosulfonate as co-products. Biotechnol Biofuels 2018;11:139.
[173] Homagain K, Shahi C, Luckai N, Sharma M. Life cycle environmental impact assessment of biochar-based bioenergy production and utilization in Northwestern Ontario,Canada. J For Res 2015;26:799–809.
[174] Smebye AB, Sparrevik M, Schmidt HP, Cornelissen G. Life-cycle assessment of biochar production systems in tropical rural areas: comparing flame curtain kilns to other production methods. Biomass Bioenergy 2017;101:35–43.
[175] Sepúlveda-Cervantes CV, Soto-Regalado E, Rivas-García P. Technical-environmental optimisation of the activated carbon production of an agroindustrial waste by means response surface and life cycle assessment. Waste Manag Res 2018;36(2):121–30.
[176] Dutta B, Raghavan V. A life cycle assessment of environmental and economic balance of biochar systems in Quebec. Int J Energy Environ Eng 2014;5:106.
[177] Sparrevik M, Field JL, Martinsen V, Breedveld GD, Cornelissen G. Life cycle assessment to evaluate the environmental impact of biochar implementation in conservation agriculture in Zambia. Environ Sci Technol 2013;47:1206–15.
[178] Hammond J, Shackley S, Sohi S, Brownsort P. Prospective life cycle carbon abatement for pyrolysis biochar systems in the UK. Energy Pol 2011;39:2646–55.
[179] Dou X, Zeng G, Ai N, et al. Life cycle assessment of greenhouse gas emissions ofSargassum Horneri-ba d ctivated carbon. Environ. Sci. Technol. (Chinese) 2015; 38(12):262–6.
[180] Hamedani SR, Kuppens T, Malina R, Bocci E, Colantoni A, Villarini M. Life cycle assessment and environmental valuation of biochar production: two case studies in Belgium. Energies 2019;12(11):2166.
[181] Lefebvre D, Williams A, Kirk G, Meersmans J, Smith P. An anticipatory life cycle assessment of the use of biochar from sugarcane residues as a greenhouse gas removal technology. J Clean Prod 2021;312:127764.
[182] Papageorgiou, A. Azzi, E.S., Enell, A., Sundberg, C. Biochar produced from wood waste for soil remediation in Sweden: Carbon sequestration and other environmental impacts. Sci Total Environ 2021;776:145953.
[183] Tadele D, Roy P, Defersha F, Misra M, Mohanty AK. Life Cycle Assessment of renewable filler material (biochar) produced from perennial grass (Miscanthus). AIMS Energy 2019;7(4):430–40.
[184] Struhs E, Mirkouei A, You Y, Mohajeri A. Techno-economic and environmental assessments for nutrient-rich biochar production from cattle manure: a case study in Idaho, USA. Appl Energy 2020;279:115782.
[185] Nie Y, Bi X. Life-cycle assessment of transportation biofuels from hydrothermal liquefaction of forest residues in British Columbia. Biotechnol Biofuels 2018;11: 23.
[186] Sevilla M, Fuertes AB. Sustainable porous carbons with a superior performance for CO_2 capture. Energy Environ Sci 2011;4:1765–71.
[187] Sun X-D, Yuan X-Z, Jia Y, Feng L-J, Zhu F-P, Dong S-S, et al. Differentially charged nanoplastics demonstrate distinct accumulation in *Arabidopsis thaliana*. Nat Nanotechnol 2020;15:755–60.
[188] Molina-Besch K. Food delivery packaging and tableware waste. Nature Food 2020;1:531–2.